VARIATION OF DRAG COEFFICIENT ON ROUGH CYCLINDRICAL BODIES

A Dissertation Submitted in Partial Fulfillment of the Requirements for the Degree of

Master of Technology
In
Civil Engineering

MONALISA MALLICK

DEPARTMENT OF CIVIL ENGINEERING
NATIONAL INSTITUTE OF TECHNOLOGY ROURKELA
2014

VARIATION OF DRAG COEFFICIENT ON ROUGH CYCLINDRICAL BODIES

A

Dissertation

Submitted in Partial Fulfilment of the Requirements for the Degree Of

MASTER OF TECHNOLOGY

IN

CIVIL ENGINEERING

WITH SPECIALIZATION IN

WATER RESOURCES ENGINEERING

Under the supervision of

Prof Awadhesh Kumar

Submitted By

MONALISA MALLICK

(ROLL NO. 212CE4489)

DEPARMENT OF CIVIL ENGINEERING

NATIONAL INSTITUTE OF TECHNOLOGY ROURKELA

2014

National Institute of Technology

Rourkela

CERTIFICATE

This is to certify that the thesis entitled, "***VARIATION OF DRAG COEFFICIENT ON ROUGH CYLINDRICAL BODIES***" submitted by Monalisa Mallick in partial fulfilment of the requirements for the award of **Master of Technology** Degree in **Civil Engineering** with Specialization in "**WATER RESOURCES ENGINEERING**" at National Institute of Technology, Rourkela, is an authentic work carried out by her under my supervision and guidance.

To the best of my knowledge, the matter embodied in this Project Report has not been submitted to any other University/Institute for the award of any Degree or Diploma.

Prof. Awadhesh Kumar
Water Resources Engineering,
Department of Civil Engineering
National Institute of Technology, Rourkela
Odisha, India

Place: Rourkela
Date: 30.05.2014

ACKNOWLEDGEMENTS

A complete research work can never be the work of anyone alone. The contributions of many different people, in their different ways, have made this possible.

First of all, I would like to express my sincere gratitude to my supervisor Prof. Awadhesh Kumar, for his guidance, motivation, constant encouragement, support and patience during the course of my research work. I truly appreciate and value his esteemed guidance and encouragement from the beginning to the end of the thesis

I wish to express my sincere gratitude to Dr. S K Sarangi, Director, NIT, Rourkela for giving me the opportunities and facilities to carry out my research work.

I would like to thank Prof. Nagendra Roy; Head of the Dept. of Civil Engineering, National Institute of technology, Rourkela. I am also thankful to Prof. Kanhu Charan Patra, Prof. Ramakar Jha, and Prof. Kishanjeet Kumar Khatua for their kind cooperation and necessary advice.

A special words of thanks to Abinash, who supported me in writing, and incented to strive towards goal.

I am also thankful to staff members of Hydraulic machine Laboratory especially Mr. Kulamani Patra and Mr. Minz for their assistance &co-operation during the exhaustive experiments in the laboratory. I express to my special thanks to my dear friends Chita, Bibhuti, Rajesh, Arpan, Ellora and my juniors Rajendra, Anta for their continuous support, suggestions and love.

Finally, I would like to thanks to my father Mr. Sankar charan Mallick and mother Mrs. Sushilabala Mallick, who taught me the value of hard work by their own example. I would like to a special thanks to my family, words cannot express how grateful I am to my Father, Mother, sweet Brother Swarop Ranjan Mallick and lovely Sister Priyanka Mallick for all of the sacrifices that you have made on my behalf.

Monalisa Mallick

Table of Contents

List of Figures

List of Tables

List of Notations

A	Projected area
C_D	Drag coefficient
C_f	Skin friction coefficient
C_P	Pressure coefficient
D	Diameter of cylinder
e	Error
F_D	Drag force
F_L	Lift force
k	Roughness
L	Length of cylinder
M	Mass
P	Gauge pressure
P	surface pressure
p	Barometric pressure
P_a	Absolute pressure
p_0	Static pressure
P_0	Total pressure
R	Gas constant
R_e	Reynolds Number

R^2	Regression coefficient
T	Time
U	Uniform Speed
V	Velocity
X	Independent Variable
X_1	Dependent variable
ν	Kinematic viscosity
μ	Dynamic viscosity
ρ	Density
τ	Shear stress
θ	Angle of incidence in degree

ABSTRACT

The accurate assessment of drag force on bodies of different configuration enable us better design of structures like buildings, chimney, towers, aeroplanes, automobiles etc. Drag coefficient is a function of speed, flow direction, object position, object shape and size, fluid density and fluid viscosity. Many factors affect the overall drag coefficient for vehicles, such as the following: (1) the shape of the bodies (leading and trailing edges), or nose, of the vehicle. (2) The surface roughness of the bodies. (3) Such appendages as mirrors, door handles, antennas, and so forth. Drag is a function of relative speed, flow direction, placement of the object, object configuration (shape and size), fluid density, fluid viscosity and roughness of the surface of the bodies. There have been persistent efforts to decrease the above problems by the use of drag force and pressure distribution of cylindrical bodies. A review of literature reveals that some investigations relating to aerodynamics quality have been carried out in cylindrical bodies. Although these examinations have thrown some graceful on the performance of definite conclusions (qualitative /quantitative) have not been arrived at as regards their improved performance on a comparative basis with respect to a conventional drag force. The literature provides limited quantitative study on the effect of roughness on related parameters in cylindrical bodies' viz. different diameter of cylinder, different size of roughness and free streamed velocity.

The present work is the result of extensive experimentation on cylindrical bodies with varying cylinder diameters, surface roughness and air velocity. The experimental variables include cylinders of diameters as 12.5mm, 15 mm, 20 mm, and 25 mm, air velocity range is 26.14, 25.48, 24.10, 23.38, 22.26, 21.87, 19.39, 15.46, 10.12 and 8.26 m/s and surface roughness as 325 micron, 260 micron, 200 micron and 160 micron. The drag coefficient of flow in each case was calculated from the data obtained by performing tests on an air flow bench (AF12). For a particular run, the value of drag force and hence the co-efficient of drag was obtained by two methods: (i) direct application of weights to counter balance the drag force and, (ii) measuring pressure at different angles around the periphery of the cylinder. The same procedure is repeated by varying, diameter of the cylinder, free stream velocity and the roughness of the surface of the cylinder.

A comparison for the drag co-efficient and pressure distribution between the smooth and rough surfaces of the cylinders are extensively presented. In case of smooth surface cylinder, the separation angles for different diameter of cylinder calculation are found to be around 80^0~90° on either side of the cylinder from the upstream stagnation point. The drag

coefficients for smooth surface of different diameter cylinders are calculated by experimentation and subsequent changes in drag due to introducing surface roughness are demonstrated. The surface roughness is found by experimentation of different drag coefficient. From the drag force data obtained from direct weighing method, the correlations both in terms dimensional and dimensionless parameters have been developed. The predicted values of drag force have been compared (graphically and tabular form) with the corresponding experimental ones and have been found to be in good agreement in the range of the experiment.

In dimensional correlation result is very sensitive, accurate and deterministic. In dimensionless correlation result is linear with their parameters.

KEYWORDS: Cylinder, Drag force, Drag coefficient, Pressure coefficient.

CHAPTER I
INTRODUCTION

1.1 AERODYNAMICS

Drag is the heart of aerodynamic design. The resistance of a body as it moves through a fluid is of great technical importance in hydrodynamics and aerodynamics. The study of the performance of bodies in moving airstreams is called aerodynamics. Hydrodynamics is the name given to the study of moving bodies immersed in liquids, particularly water. Drag force reduces fuel consumption, range and speed. (Grosche and Meier in 2001) The basic principle of drag reduction for automobiles include providing rounded smooth contours for the forward part, elimination or streamlining of appendages, blending of changes in contour (such as at the hood/windshield interface), and rounding of rear corners. Decreasing drag is a major goal in designing most kinds of vehicles because a significant amount of energy is required to overcome drag as vehicles move through fluids (Tsutsui and Igarashi in 2002). Drag coefficient is a function of speed, flow direction, object position, object shape and size, fluid density and fluid viscosity. Many factors affect the overall drag coefficient for vehicles, such as the following:

1. The shape of the bodies (leading and trailing edges), or nose, of the vehicle.
2. The surface roughness of the bodies.
3. Such appendages as mirrors, door handles, antennas, and so forth.

Drag coefficient is not a constant term. It is a function of relative speed, flow direction, placement of the object, object configuration (shape and size), fluid density, fluid viscosity and roughness of the surface of the bodies. When simulating the wind flow over a scale model comprised of curved surfaces, discrepancies are present between the

model scale data and full scale winds experienced by the structure. Since the Reynolds number corresponding to the curved surface is a function of the radius of curvature, there is an inconsistency between the model scale Reynolds number and the full scale Reynolds number.

For a circular cylinder, Reynolds number can be computed via Equation (1.1).

$$R_e = \frac{vd}{\nu} \tag{1.1}$$

Where, R_e is the Reynolds number of the shape; v is the wind velocity in unobstructed flow, d is the diameter of the cylinder and ν is the kinematic viscosity of air.

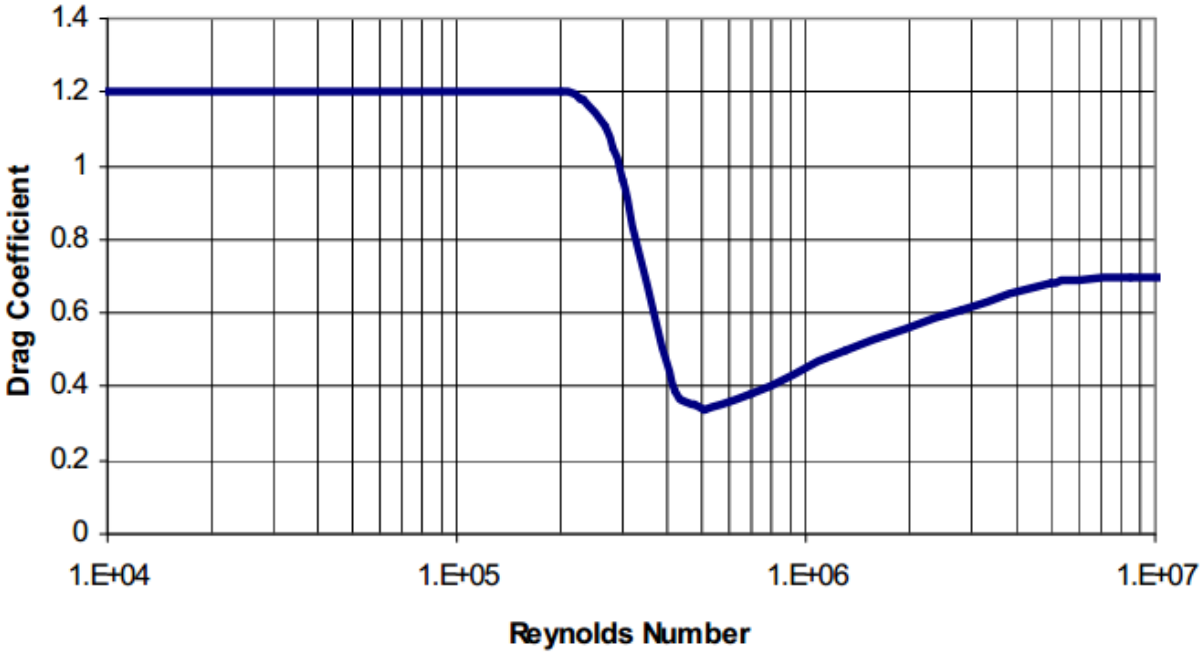

Drag coefficient vs. R_e number for a circular cylinder (Scruton and Rogers, 1971).

Fig. 1.1 Drag coefficient vs Reynolds number for a circular cylinder

Subcritical flow over a smooth cylinder generally occurs at R_e less than $2x10^5$ Sub-critical flows are characterized by laminar flow over the windward surface of the cylinder with the

flow separating on the upwind face (Scruton and Rogers in 1997). Super-critical flow occurs at R_e greater than $4x10^6$ and is evident by the turbulent boundary layer that forms over the surface of the cylinder. The turbulent wind separates from the cylinder on the leeward face and results in a lower drag coefficient. The critical region is defined as flow resulting at R_e between those of sub-critical and super-critical flows. Aerodynamic drag generally consists of friction drag and pressure drag. Friction drag is determined almost entirely by the state of the boundary layer (laminar, transition or turbulent), and does not vary greatly between subsonic and supersonic flight.

1.2 FLOW CLASSIFICATION

Flow velocity is used to classify flows according to speed regime. Subsonic flows are flow fields in which air velocity throughout the entire flow is below the local speed of sound. Transonic flows include both regions of subsonic flow and regions in which the flow speed is greater than the speed of sound. Supersonic flows are defined to be flows in which the flow speed is greater than the speed of sound everywhere. A fourth classification, hypersonic flow, refers to flows where the flow speed is much greater than the speed of sound. Aerodynamicists disagree on the precise definition of hypersonic flow. (Pasto in 2008)

1.2.1 Subsonic Flow

Subsonic (or low-speed) aerodynamics studies fluid motion in flows which are much lower than the speed of sound everywhere in the flow. There are several branches of subsonic flow but one special case arises when the flow is in viscid, incompressible and irrational. This case is called potential flow.

1.2.2 Transonic flow

The term Transonic refers to a range of velocities just below and above the local speed of sound (generally taken as 0.8-1.2). It is defined as the range of speeds between the critical Mach number, when some parts of the airflow over an aircraft become supersonic and a higher speed, typically near Mach 1.2, when all of the airflow is supersonic. Between these speeds, some of the airflow is supersonic, and some is not.

1.2.3Supersonic flow

Supersonic flow behaves very differently from subsonic flow. Fluids react to differences in pressure; pressure changes are how a fluid is "told" to respond to its environment. Therefore, since sound is in fact an infinitesimal pressure difference propagating through a fluid, the speed of sound in that fluid can be considered the fastest speed that "information" can travel in the flow.

1.2.4 Hypersonic flow

In aerodynamics, hypersonic speeds are speeds that are highly supersonic. In the 1970s, the term generally came to refer to speeds of Mach 5 (5 times the speed of sound) and above. The hypersonic regime is a subset of the supersonic regime. Hypersonic flow is characterized by high temperature flow behind a shock wave, viscous interaction, and chemical dissociation of gas.

1.3 DRAG ON A CYLINDER

The drag force i.e. the force exerted by the following fluid on the cylinder in direction of flow depends upon the Reynolds number of the flow. From experimentations, it has been observed that:

(i) When Reynolds number$(R_e) < 1$, drag force is directly proportional to velocity and hence the drag co-efficient (C_D) is inversely proportional to Reynolds number.

(ii) When Reynolds increases from 1 to 2000, the drag co-efficient decreases. The minimum value of 0.95 at R_e = 2000.

(iii) When the value of Reynolds number is increased from 3×10^4 to3×10^5. At $R_e = 3 \times 10^5$, the value of C_D is 0.3.

(iv) If the Reynolds number is increased beyond3×10^6, the value of C_D increases and it becomes equal to 0.7 in the end.

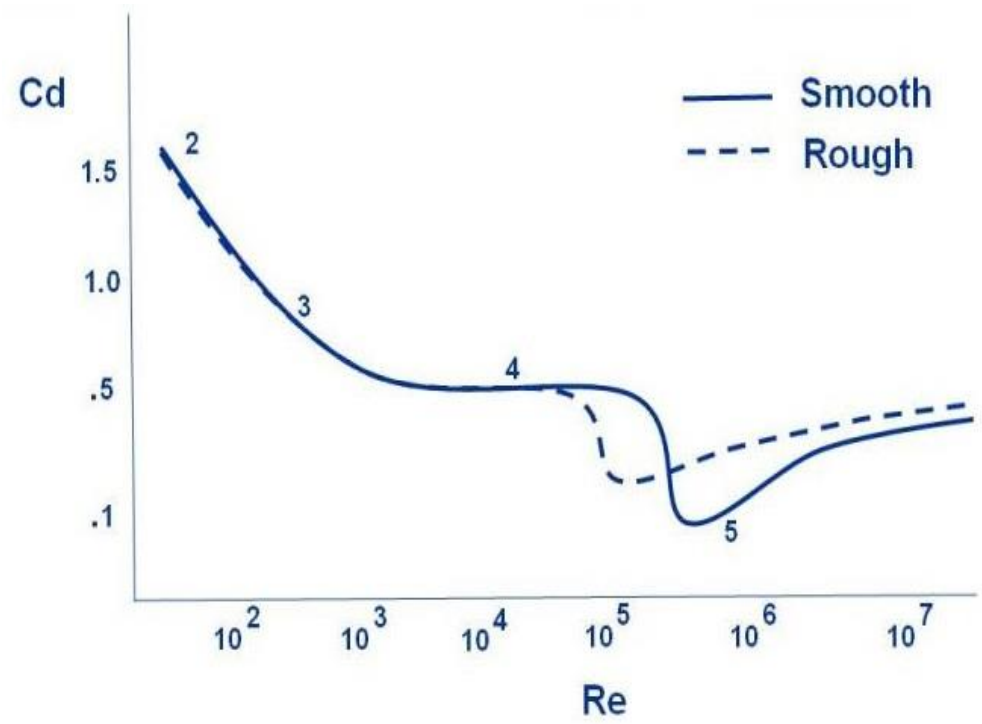

Fig. 1.2 Drag coefficient vs Reynolds number for a smooth surface cylinder and rough surface cylinder.

1.4 DRAG

The component of the total force in the direction of motion is called drag. Thus drag is the force exerted by the fluid in the direction of motion. Drag is the force on a body caused by the fluid that resists motion in the direction of travel of the body.

1.5 LIFT

The component of the total force in the direction perpendicular to the direction of motion is called lift. Thus lift is the force exerted by the fluid in the direction perpendicular to the direction of motion.

1.6 DRAG FORCE

The drag force = Force due to pressure in the direction of fluid motion and force due to shear stress in the direction of fluid motion.

$$= \mathrm{p}dA\cos\theta + \tau_0 dA\cos(90-\theta) \tag{1.2}$$

Total Drag

$$F_D = \mathrm{p}dA\cos\theta + \tau_0 dA\sin\theta \tag{1.3}$$

1.6.1 Pressure Drag and Friction Drag

Total drag on a body is due to two components. Pressure drag (also called form drag) is due to the disturbance of the flow stream as it passes the body, creating a turbulent wake. Friction drag (also called skin drag and shear drag) is due to shearing stresses in the thin layer of fluid near the surface of the body called the boundary layer.

The relative contribution of the pressure drag and friction drag to the total drag depends on:

1. Shape of the immersed body.

2. Position of the body immersed in the fluid, and

3. Fluid characteristics.

1.7 DRAG COEFFICIENT

- The magnitude of the drag coefficient for pressure drag depends on many factors, most notably the shape of the body, the Reynolds number of the flow, the surface roughness, and the influence of other bodies or surfaces in the vicinity.
- It is a dimensionless number that depends on the shape of the body and its orientation relative to the fluid stream.
- C_D is the drag coefficient.

1.8 PRESSURE COEFFICIENT

- C_P is the pressure coefficient.
- Experimental procedure is to measure C_P at different angular position on the surface of the cylinder to predict the overall drag coefficient and separation angle of the cylinder.
- $C_P = \frac{P-p_0}{\frac{1}{2}\rho U^2}$ (1.4)

1.9 SIGNIFICANCE AND OBJECTIVES FOR THE RESEARCH

The present work is aimed to study the distribution of pressure in 'rough cylindrical bodies'. The distribution of pressure along the cylinder depends on total pressure, static pressure, pressure coefficient, angle of incidence and free streamed velocity. Out of these parameters

pressure coefficient and angle of incidence plays a major role in estimation of pressure distribution in rough cylindrical bodies.

Even for rough cylindrical bodies computational works are reported more than experimental studies. Therefore experimental analysis on drag force along the rough cylindrical bodies can be studied more extensively which can further applied to automobile during aerodynamic conditions. These studies should be useful in determining the drag coefficient through a rough cylindrical body to solve many designing problems and also it provides a better design of structure in automobiles, building and towers. The objectives of the present work are summarized as:

1. To Measure the drag force on cylindrical bodies with varying velocity, diameter and roughness.
2. To measure pressure distribution at (0 to 180, and 0 to -180) angles of incidence for the different cases. Determination of pressure distribution along with different diameter and different size of roughness in cylindrical bodies.
3. To find out drag coefficient under varying above varying conditions by two methods viz. (i) Drag force by direct weighing method and (ii) pressure measurement at different angles of incidence.
4. To compare predicted values of drag co-efficient with the corresponding ones obtained experimentally by above two methods.
5. To propose a correlation for the drag co-efficient. Development of a correlation with dimensionless and dimensional analysis of the drag force and drag coefficient of the cylindrical bodies.

6. To conduct experiment and analyze experimental data for the investigation of drag force and pressure distribution for different diameter, roughness and velocity for smooth and rough cylindrical bodies.

1.10 ORGANISATION OF THESIS

The thesis consists of seven chapters. General introduction is given in Chapter 1, literature review is presented in Chapter 2, experimental work is described in Chapter 3, experimental results are outlined and analysis of results are done in Chapter 4, the dimensionless correlation is in chapter 5, the development of correlation is in chapter 6 and finally the conclusions, scope of future work and references are presented in Chapter 7.

Chapter-1 outlines the introduction to different characteristic of drag force along with their impact on the drag coefficient and pressure distribution phenomenon and the objectives of the investigation undertaken.

Chapter–2 presents the literature review which summarizes the up-to-date investigations related to drag coefficient viz. drag force, pressure coefficient, pressure distribution, surface roughness and drag reduction. Investigations in drag force with various shape and size specification and supported by different types of coefficient have also been incorporated in this chapter.

Chapter–3 describes the experimental setup with details of attachments: one for Direct weighing method and another for pressure distribution. It also explains detailed experimental procedure and methodology. The different aspects of investigation have also been outlined. The variables include cylinders of four diameters, four different roughness for the cylindrical

surfaces and ten free stream velocities. The scope of the present investigation has been presented in **Table No-3**.2

Chapter- 4 presents data collection and analysis. The calculation of drag coefficient ratio (C_D) i.e. the ratio of the drag force and $\frac{1}{2}\rho A v^2$. Thus, drag coefficient ratio is a function of drag force and dynamic pressure of the cylindrical bodies.

The comparison of the predicted results for the drag force ratio for the drag force and dynamic pressure indicates that all types of diameters used in the investigation are quite effective in reducing the roughness over the drag force ones. Also, the effect of the pressure coefficient results in the reduction of drag coefficient. Thus, the combined effect of roughness, velocity and diameter and pressure coefficient, whereas diameter increases the drag force increases and velocity increases the drag force increases, velocity decreases with drag force decreases.

Chapter- 5 Presents the development of two correlations: (i) in dimensional terms and (ii) in the in non-dimensional forms. The relation can be expressed as functions of dimensionless terms containing roughness, velocity and diameter parameters and the properties of the aerodynamic particles and the aerodynamic medium. These correlations have been expressed in the form of modified drag coefficient ratio (C_D) in order to ensure the analysis of the experimental data for the effect of the individual dimensionless group has been carried out. Using the values of the constants and the exponents as obtained by the regression analysis of the data, the final correlations for modified drag coefficient ratio have been obtained as under: For this, drag coefficient ratio has been expressed as functions of system variables in dimensional and non-dimensional forms separately as under:

(i) Dimensional terms: $F_D = C(V^{n_1})(D^{n_2})(k^{n_3})$

(ii) Dimensionless terms: $\frac{F_D}{\frac{1}{2}\rho AV^2} = C(Re)^{n_1}\left(\frac{k}{D}\right)^{n_2}$

Developed for the prediction of drag force in rough cylindrical bodies with different diameter of cylinder and different surface roughness. To show the effect of roughness, effect of velocity, effect of diameter. The developer parameters have been used in dimensionless form and the following correlations have been developed:

Chapter -6 Using different system variables expressed in dimensionless form, the following correlations have been obtained:

Chapter-7 conclusion summarizes the conclusion reached by the present research and scope of future work is listed out.

References that have been made in subsequent chapters are provided at the end of the thesis.

CHAPTER II
REVIEW OF LITERATURE

2.1 GENERAL

Although the literature covers an extensive variety of theories, this review will focus on major theories which develop constantly. The Chapter describes the past research works based on the proposed study. A continuous effort has been made researchers to study the pressure drag and shear drag on different bodies. The widespread use of drag coefficient in aerodynamic applications has motivated many researchers to study various characteristics of their geometrical parameters. Drag force along the drag coefficient of a cylinder is influenced by Many factors particularly, the different diameter of cylinder, velocity and the size of the roughness i.e. 326 micron, 260 micron, 200 micron, 160 micron. It is quite necessary to take into description the pressure distribution that exists in aerodynamics to understand the pressure coefficient. So the present review of literature includes works on experimental research of pressure distribution and drag coefficient for rough cylindrical bodies in aerodynamics.

2.2 REYNOLDS NUMBER FOR CIRCULAR CYLINDER

Many researches had been carried out to predict the variation of drag Coefficient vs. Reynolds number for circular cylinder.

***Roshko* (1961)** showed that measurements on a large circular cylinder in a pressurized wind tunnel for Reynolds numbers from 10^6 to 10^7 and revealed a high Reynolds number transition in which the drag coefficient increases from its low supercritical value to a value

0.7 at R_e = 3.5 x $l0^6$ and then becomes constant. Also, for R_e > 3.5 x $l0^6$, definite vortex shedding occurs, with Strouhal number 0.27.

Achenbach and Heinecke **(1981)** observed that the range of Reynolds number 6×10^3 to 5×10^6 effect of relative roughness on drag for the flow over circular cylinder. They investigated vortex shedding phenomena in this range.

Shih and Wang et al **(1993)** studied the flow past rough circular cylinders at high Reynolds numbers. In their research they had carried out experiments using three rough cylinder models with three different k/d ratios, along with one smooth cylinder. They had tested using variable density, low turbulence facilitated pressure tunnel at NASA Ames Research Centre. It is found that there is an effect of Reynolds number on pressure distribution at low R_e and hence for all three roughness model and smooth model, the base pressure co-efficient depends on Reynolds number. When the roughness increases, the base-pressure co-efficient becomes independent of Reynolds number in the range beyond $2x10^6$.

Williamson **(1996)** has presented comprehensive description of flow phenomena at different Reynolds number.

Mittal and Singh **(2005)** studied flow past a circular cylinder for Re= 10^0 to 10^7 numerically by solving the unsteady incompressible two dimensional Navier-Stokes equations and they described the shear layer instability and drag crisis phenomena.

Triyogi et al. **(2009)** used of the I-type small cylinder with a cutting angle of $\theta s = 65^\circ$ as passive control at a stagger angle of $\alpha=0$ is most effective in reducing the drag of the large circular cylinder, among the passive control cylinders used in this investigation.

Butt and Egbers **(2013)** presented that a circular cylinder produces large drag due to pressure difference between upstream and downstream. The difference in pressure is caused by the

periodic separation of flow over surface of the cylinder. In this paper, discussed taking into consideration the well-known characteristics of flows over rough and dimpled cylinders and flow over circular cylinders with patterned surfaces is studied. Researches were performed in a subsonic wind tunnel to note the effect of hexagonal patterns on the flow of air at Reynolds numbers ranging from 3.14E+04 to 2.77E+05. The investigations shown that a patterned cylinder with patterns pressed outwards has a drag coefficient equal to 65% of the smooth one. Various flow visualization techniques including measurement of velocity profiles in the wake region and smoke flow visualization were employed to explain the effect and hence understand the reason of drag reduction. Besides that the investigation of vortex shedding frequencies determined by using hot wire anemometry suggested that they do not change expressively with the decrease in drag coefficient in contrast to the dimpled cylinders.

2. 3 DRAG REDUCTION OF A CIRCULAR CYLINDER

***Bouak and Lemay* (2001)** the value obtained for the single cylinder is about 32% less than of the reduction of mean drag coefficient by claimed other authors. This result gained at R_e values ranging from 1.5×10^4 to 4.0×10^4,S/d=2.55,and ds/d=1.25.

***Grosche and Meier* (2001)** this paper summaries nearly experimental investigations on aerodynamics of bluff bodies which had been carried out at the former DLR Institute of Fluid Mechanics, now Institute of Aerodynamics and Flow Technology. (a) drag reduction by passive ventilation of the wake of the body, (b) reduction of the drag of automobiles by shape optimisation to eliminate or at least decrease trailing vortices, (c) determination of the main sources of aerodynamic noise of high velocity trains which result from unsteady flow

separations, (d) experiments on active flow control to delay flow separation are included given.

Tsutsui and Igarashi **(2002)** Studied that drag reduction of a circular cylinder in an air-stream is studied the flow characteristics of a bluff body cut from a circular cylinder. Two types of test models were employed in their study and States that the distributions of C_p are practically symmetric for all the small cylinders tested (circular or sliced). The value of C_p at the front region was close to zero or a negative value. This is because a quasi-static vortex is formed between the I-type small cylinder and large cylinder as by and C_p has a maximum of 0.1–0.2 at the reattachment region of the shear layer separated from the small cylinder. The bluff body cut from a small circular cylinder that is cut at both sides parallel to they-axis was used as passive control to reduce the drag of a larger circular cylinder. The small bluff body cut is called an I-type bluff body, which interacts with a larger one downstream. I-type bluff bodies with different cutting angles of θs =0˚(circular), 10˚,20˚,30˚,45˚,53˚, and 65˚were located in front and at the line axis of the circular cylinder at a spacing S/d=1.375, where their cutting surfaces are perpendicular to the free stream velocity vector. The tandem arrangement was tested in a subsonic wind tunnel at a Reynolds number (based on the diameter d of the circular cylinder and free stream velocity) of R_e=5.3×104. The results show that installing the bluff bodies (circular or sliced) as a passive control in front of the large circular cylinder effectively reduces the drag of the large cylinder. The passive control with

cutting angle θs =65◦gives the highest drag reduction on the large circular cylinder situated downstream. It gives about 0.52 times the drag of a single cylinder.

Alma and Moriya **(2003)** The goal of this study was on the determination of the characteristics of steady and wake frequencies, fluctuating fluid forces and switching

phenomena in two side-by-side cylinders. In the case of corresponding vortex shedding and even in the transitional flow pattern, a predominant antiphase corresponding vortex was found in both the case of two side-by-side circular cylinders and the case of two side by-side square cylinders. For T=D>0:20; (T; gap spacing between cylinders; D; diameter), the action of lift forces on both cylinders was in an outward (repulsive); however, for T=D¼0:10; the action of lift force on the cylinder related with the narrower wake was inward and that on the other cylinder was outward. The aerodynamic characteristics of two stationary cylinders, both square and circular, in a side-by-side arrangement were examined experimentally in a uniform flow at a Reynolds number of 5.51×10^4, although the square cylinder results are partial.

***Lee and Cheol* (2004)** Flow control around bluff bodies is of importance and of interest for wind engineering. The authors investigated this flow control and proposed two new flow control methods. The first method controls shear layers separated from the bluff body, and the second controls surface flow around bluff bodies by setting up a small rod upstream of the bluff body. For the second method, the authors stated that the flow pattern changes, depending on rod diameter ds, its position, and Reynolds number. For Reynolds numbers Re ranging from1.5×10^4 to 6.2×10^4 and the ratio of rod diameter relative to downstream cylinder diameter (ds/d) being 0.25, with the longitudinal distance between the axis of the

downstream cylinder to the rod relative to downstream cylinder diameter(S/d) being 1.75–2.0, the total drag including the drag of the rod decreased by 63 per cent compared with that of a single cylinder.

***Pasto* (2008)** presented the results of experimentation on the behavior of a freely vibrating circular cylinder in laminar and turbulent flows. By varying the cylinder roughness and the

mass-damping parameters wind tunnel tests had been conducted. The effects of surface roughness and flow turbulence were considered in term of an effective Reynolds number, Re eff. Here it was seen that, it was possible to examine the sample before and after the beginning of the cylinder boundary layer transition. It had been shown that both mz and Reynolds number play an important role in governing the response during lock in; If mz is fixed, the responses is inversely related to Re_{eff} , i.e. with increase in responses the value of Re_{eff} decreases and vice versa. Moreover, it had been observed that the cylinder may experience vortex-induced vibrations even in the critical Re_{eff} regime characterized by a cessation of coherent vortex shedding in steady configuration. They discussed about the effects of mz and Re_{eff} on the critical velocity (the velocity at which the maximum amplitude of response is approached), on the wideness of the lock in range, and on the wake correlation length.

Mohammad and Islam et al. **(2010)** Drag indicates a great role on aerodynamics and fluid mechanics while it is shown for any kind of moving object of different shape. An important number of experiments were achieved for reduction of drag force because drag causes high power consumption and also structural failure of the object. Reduction of drag force of circular cylinder by attaching circular rings is described in this research. For finishing this experiment models are verified in 36x36x100 cm subsonic wind tunnel. By using an external balance, drag measurements are carried out. Drag force over circular cylinders of different diameter without any rings are verified first. Then circular rings attached circular cylinders are verified. It is observed that there is reduction of drag even though the projected area increased because rings causes more attached flow than the plain cylinder. The optimum value of drag reduction is found when ring is 1.3d and aspect ratio of cylinder is

approximately 12. The experimental results show drag reduced by this optimum configuration is 25%.

Guy and Steve **(2012)** presented the result of an investigation on the effect of wind turbulence for the reduction of drag for a speed skater. A speed skater competing in an indoor oval is subjected to turbulent flow condition. The goal of the research is to calculate drag coefficients for different Reynolds numbers. The goal of the report is to identify the characteristics of different drag coefficient on bluff body aerodynamics and to show the need of slender bodies through the drag values. Circular cylinder has large dynamic drag resulting from the separation of flow over the cylinder. To reduce the drag coefficient of a circular cylinder, some methods have been studied, such as a cylinder with roughened surface, and so on.

Tamayol **(2013)** studied that Pressure drop of ordered arrays of cylinders embedded inside micro channels was experimentally and methodically. Two independent modeling techniques are used to predict the flow resistance for the creeping flow regime. The pressure drop is expressed as a function of the involved geometrical parameters such as micro-cylinder diameter, spacing between adjacent cylinders, channel height, and its width. To verify the developed models, 15 silicon/glass samples are fabricated using the deep reacting ion etching (DRIE) technique. Pressure drop measurements are performed over a wide range of nitrogen flow rates spanning from 0.1 sccm to 35 sccm. Both methods predict the trend of the experimental data. The porous medium approach shows a wider range of applicability with reasonable accuracy while the variable cross-section technique is more accurate for dense arrays of micro-cylinders. Our results suggest that an optimal micro-cylinder diameter exists that minimizes the pressure drop for a specific surface area-to-volume ratio. This diameter is a function of the channel dimensions and the desired surface area-to-volume ratio.

2.4 PREVIOUS WORKS ON EXPERIMENTAL RESEARCH FOR DRAG COEFFICENT

The literature review contains cylindrical bodies of research on the subject of drag force in aerodynamics. This review intends to present some of the selected significant contribution to the study of drag force in aerodynamics. Research are done covering several aspects such as using different shape like cylinder and flat plate; different size of cylinder such as 0.0125m, 0.015m, 0.020m, 0.025m with different surface types like smooth and rough cylinder to study the factors influencing the drag force and pressure distribution.

***Alridge and Hunt* (1978)** Measurements are described of the drag coefficient of porous circular cylinders fixed between solid hemispherical end caps, for five values of aspect ratio between 7.92 and 2.67 .The Reynolds number varies between 10^4 and 2.6 $xl0^5$. It is found that the drag coefficient increases with aspect ratio much as a solid cylinder's but its drag coefficient is about 20% higher. Flow-visualization experiments have also been conducted, and show how fluid passes through the cylinders and how the vortex shedding is weaker than for solid cylinders.

***Protas* (2002)** we are absorbed in identifying the physical mechanisms that accompany mean drag modifications in the cylinder wake flow subject to rotary control in this paper. We studied simple control laws where the obstacle rotates harmonically with frequencies varying from half to more than five natural frequencies. In our analysis we studied the results of the numerical simulations at Re=150. All the simulations were performed using the vortex method. We confirm the concerning mean drag reduction at higher forcing frequencies. The main result is that changes of the mean drag are achieved by modifying the Reynolds stresses

and the related mean flow correction. It is argued that mean drag reduction is connected with control driving the mean flow toward the unstable the basic flow.

***Richter and Petr* (2012)** the heat and fluid past non-spherical particles under different angles of attack is measured. They investigated drag forces for spherical and non-spherical particles works about the nusselt number relations for non-spherical particles are rare. The angle of attack in semi-empirical models, published correlations for drag coefficient and nusselt number are improved and the accuracy of closures developed for drag coefficient and nusselt number is discussed in a comparison with published models.

2.4.1 Cylindrical Bodies

***Mittal and Balachander* (1995)** described the effect of three dimensionality on the lift and drag of nominally two-dimensional cylinders which is useful to describe the variation of numerical results between two dimensional and three dimensional analysis.

***Michel Bergmann and Laurent Cordier* (2007)** investigated the optimal control approach for the active control of the cylinder wake flow considered in the laminar (Re =100). The main

objectives is the minimization of the mean total drag where the control function is the time harmonic angular velocity of the rotating cylinder.

***Z.C. Zheng and N. Zhang* (2008)** studied frequency ranges to be considered are both near and away from the natural frequency of wake vortex shedding. Consequently, the effects of frequency lock-in, superposition and de multiplication on lift and drag are conversed based on the spectral analysis of time pasts of lift and drag. A transversely oscillating cylinder in a uniform flow is modeled to investigate frequency effects of flow-induced wake on lift and drag of the cylinder. Definitely, shown unsteady fluid dynamic simulations using an immersed-boundary method in a fixed Cartesian grid predict the flow structure around the

cylinder and reveal how the integration of surface pressure and shear distributions provides lift and drag on the oscillating cylinder.

2.4.2 Rough Cylindrical Bodies

N. Lyotard and Nicolas **(2007)** using a continuous ultrasound technique, determined velocity measurements of steel spheres in free fall through liquid. Alternatively, random surface roughness and/or high concentration polymer solutions reduce drag gradually and suppress the drag crisis. We also present a qualitative argument which ties the drag reduction observed in low concentration polymer solutions to the Weissenberg number and normal stress difference.

2.5 SURFACE ROUGHNESS OF CYLINDRICAL BODIES

The concept of controlling the flow over circular cylinders is not innovative, as many researchers have studied the effect of surface roughness on cylinders in the past.

Roshko **(1961)** cleared the range of critical R_e which poses the fundamental problem for the scale model testing of curved structure in low speed wind tunnels. Various experiments conducted to investigate the flow around circular cylinders. It obtained by model testing a curved structure at sub-critical R_e. In contrast, wind loads can be underestimated if a building is model tested at critical R_e.

Merrick and Girma **(1982)** some difficulties are encountered when simulating super-critical Reynolds number flow over curved surfaces of a building in a low speed boundary layer wind tunnel due to the sensitivity of the flow to Re. Surface roughness on the façade of the cylinder can affect the location of the separation point and the extent of the wake on the leeward face, upon which the wind-induced responses are dependent. This study attempts to control the

flow around a circular cylinder through the application of artificial surface roughness across the exterior of the cylinder. Later, the size of the artificial roughness will be correlated with R_e deviations through a computational fluid dynamics wind flow simulations. These correlations will support in selecting the suitable artificial roughness that will cause boundary layer transition at points similar to super-critical R_e simulations. Some roughness patterns were tested on the circular cylinders, which were subjected to wind flows with varying turbulence intensity. Measurements of the pressure distribution across the façade have been obtained over the R_e range of $1x10^4$ to $2x10^5$ in a BLWT. The results have direct application in the testing of scale models in low speed BLWTs where super-critical flow characteristics are anticipated. They described effect of surface roughness for flow over a body at high Reynolds number using wind tunnel.

Bearman and Harvey **(1993)** observed dimpled surfaces of cylinder, while roughness on a cylinder was studied Szechenyi (1975). Both of these studies presented that the pressure distribution around the cylinder was altered through the addition of a roughness pattern.

2.6 PRESSURE DISTRIBUTION

Libii and Josue **(2010)** Hands-on exercises were designed and tested in a subsonic wind tunnel to study pressure distributions around a circular cylinder in cross flow. They allowed students to collect their own data and use them to examine how the pressure on the surface of the cylinder changes with two different variables: the location of a given point along the circumference of the middle cross section of the cylinder and the magnitude of the Reynolds number of the flow. Plotted data produced curves very similar to those in the research literature. Detailed examination of results demonstrated how viscous flow behaviour in the upstream half of the cylinder differed from that on its downstream half. The influence of the

magnitude of the Reynolds number on the ability of the viscous flow to recover pressure on the downstream side of the cylinder was demonstrated.

Hodzic and Rasim **(2011)** Aerodynamics, as branch of fluid mechanics studies relative motion of air around the body from theoretical and experimental aspect. Those two approaches will not give same results if using theoretical laws based on ideal process, because experimental investigation is presentation of real Process. Wind tunnel is an instrument that can be used for experimental investigation. Results of cylinder surface pressure distribution, gained by experimental investigation in wind tunnel are presented in this paper. Obtained experimental results are compared with theoretical results, and on the basis of that data certain conclusions are brought.

Islam and Rakibul **(2013)** Flow past a stationary circular cylinder at $Re=10^5$ is studied numerically using Favre-averaged Navier-Stokes equation and solved via finite volume method. Numerical observations are compared with experimental results and with research works of other researchers. Different flow phenomena such as flow separation, pressure distribution over the surface, drag etc. are also studied at different boundary conditions. In case of smooth cylinder, the separation angles for experimentation calculation are found to be around 80~90° in either side of the cylinder from the upstream stagnation point. The drag coefficients for smooth surface are 0.771 and 0.533 for experimental calculation respectively and subsequent changes in drag due to introducing surface roughness are demonstrated. The critical surface roughness is found to be around 0.004 with coefficient of drag 0.43. They described separation angle for flow over the cylinder at low Reynolds number. They studied the effects of surface roughness on pressures and dynamic forces on a circular cylinder for the Reynolds number range of $6x10^4$ to $1x10^4$ in grid generated turbulent flows. He obtained rough cylinders by wrapping the cylinders with commercial sandpapers to

develop separated regions and pressure distributions corresponding to a higher equivalent Reynolds number on a smooth cylinder. The Reynolds number in the flow is increased by increase of wind tunnel blockage or turbulent intensity level. The mean and fluctuating pressure distributions on cylinders of different surface roughness in smooth and turbulent flow were plotted. He showed that the fluctuating pressures for the rough cylinders at different Reynolds numbers are very close to that smooth cylinder at supercritical Reynolds number. Thus he provided the database for further research on rough cylinders for Reynolds number beyond $1x10^6$.

Kumar and Pilla (2012) the fluid dynamics research and its results show the prediction of drag coefficient for lesser Reynolds number only. When Reynolds number increase may lead to change in drag with respect to subcritical, critical, and super critical. This research concentrates on the flow over the circular cylinder for high Reynolds number to the order of 10^8. The analysis has been done to predict drag and the variation of traditional C_D Vs Reynolds number curve plotted. Pressure distribution over the cylinder with respect to the angle shows the physical importance of drag value. Roughness with two cases is measured in this research wherever one is internal the circular cylinder and the next is internal roughness.

CHAPTER III
EXPERIMENTATION AND PROCEDURE

3.1. GENERAL

In our day-to-day life generally we use many things i.e. Automobiles as like motorcycles, cars, aeroplanes, ships etc. We use different shapes, different size of buildings, towers, chimneys, temples etc. Basically these are depends upon drag force. For example a vehicle is different shape, size, and design. So that it depends on drag force. Generally, experimental work based on automobiles is slightly difficult to present in a laboratory in practical point of view. For this cause a designed model of a drag force in a laboratory is required. In these experiments, we easily know that which method of experiment is more accurate to another. Many investigators have developed a number of models which partially satisfied the condition of rough cylindrical bodies. Our present study is related to development of a model which predicts a suitable model which gives more accurate drag force prediction for rough cylinders than previous. According to the requirement of the project the attachment of the airflow bench is maintained as follows.

Hydraulic mechanics Lab facilities of National Institute of Technology (NIT) was used to study the flow over the cylinder experimentally. The present research work utilises the setup of airflow bench fig.3.1 competence available in the Hydraulic Machine Laboratory of the Civil Engineering Department, at the National Institute of Technology, Rourkela, India. The basic objective behind these experiments is to imagine better understanding on the variation of drag coefficient and pressure distribution due to variation surface roughness, drag force and drag coefficient also.

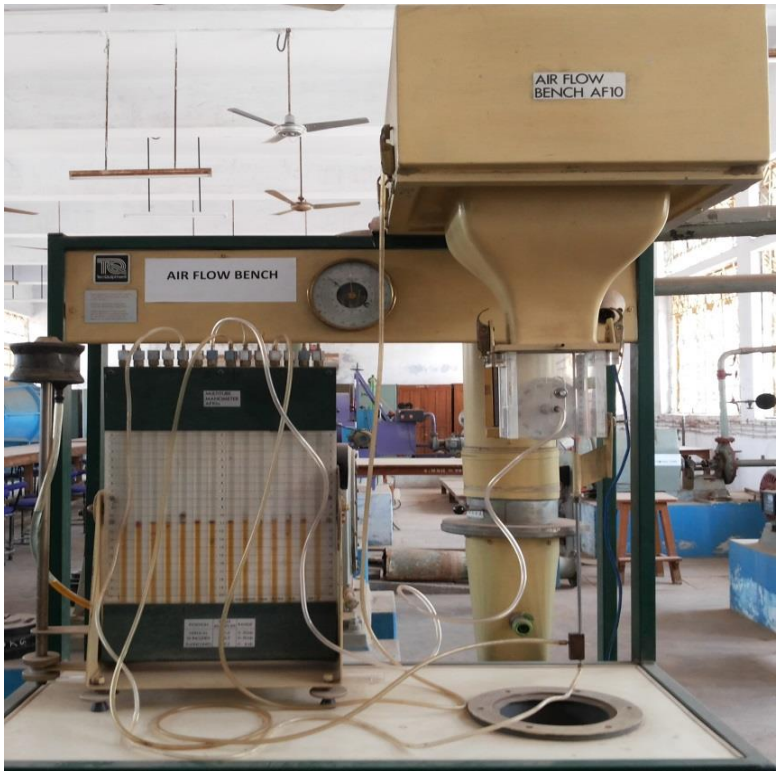

Fig. 3.1 Airflow Bench

3.2 APPARATUS & EQUIPMENTS USED

In this present study we use different diameters of cylinders like smooth surface and rough surface cylinders, weight box, one Pitot tube, and a multitube manometers were used in the experiments. These are used to measure velocity and its direction of flow in the setup. In the experiments setup like measurements of drag force and pressure distribution attachments are used. The measuring equipment and the devices were arranged properly to carry out experiments in the attachments. The apparatus used in the experimentation in both attachments, measurements of direct weighing and pressure distribution is given in the Figure 3.2 (i to iv) below.

(i) Air Temperture Meter

(ii) Multitube Manometer

(iii) Weight Boxes

(iv)Velocity Controller

Fig 3.2 (i to iv) Apparatus used in experimentation in both attachments

3.3EXPERIMENTAL PROCEDURE

In Figure 3.1, the set-up airflow bench consists of two types of attachments: (i) for drag force by direct weighing method in Figure 3.4 and (ii) drag co-efficient by pressure distribution method Figure 3.5. The setup consists of an adjusting lever to control flow, a multitube manometer for pressure measurement. This setup allowed to study of the drag of various bodies, the pressure distribution around a cylinder. Balance arm attached to the side of the main unit and holds the models in place inside the main unit. In Figure 3.3, this drag force experiments, it is used with adjustable weights and for the pressure distribution experiment, a protractor and cylinder model is fitted in the main body. The circular cylinder is connected to the separate manometer to display the pressure distribution as the cylinder is rotated.

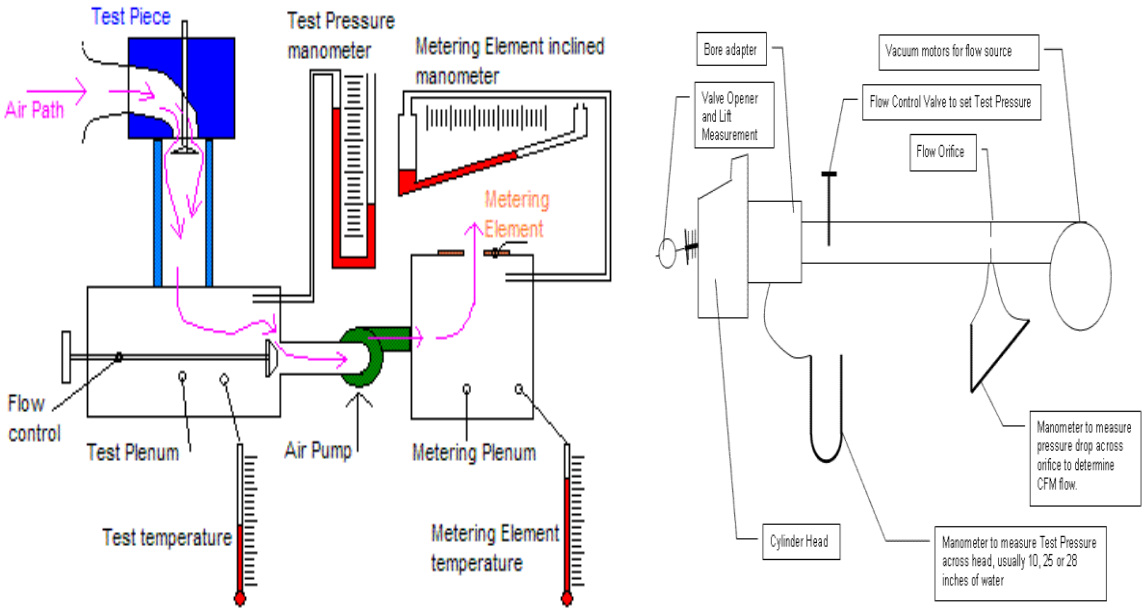

Fig.3.3 Schematic Diagram of Experimental Setup of Airflow Bench

3.4 EXEPERIMENTAL SETUP

For a particular run, the value of drag force and hence the co-efficient of drag was obtained by (i) direct application of weights to counter balance the drag force. The same procedure is repeated by varying diameter of the cylinder, free stream velocity and varying roughness of the surface of the cylinder. In Direct weighing method, we used total pressure (P0), static pressure (p0) at the inlet, pressures and the value of the weights. In this experiment, we used four different diameters and also four different size of surface roughness. i.e. 0.0125m, 0.015m, 0.020m and 0.025m diameters. 325 micron, 260 micron, 200 micron, & 160 micron surface roughness.

3.4.1 Setup for Drag Force Measurement

- Fit the circular cylinder model in position and adjust the weights to achieve equilibrium. Record the value of the weights.
- Switch on the fan and adjust the wind speed to a low level and readjust the weights to achieve equilibrium.
- Record the value of the weights and total pressure and static pressure at the inlet.
- Increases the wind speed in increments up to its maximum level, each time readjust the weights to achieve equilibrium and record the pressures and value of the weight.

Fig.3.4 Setup for Drag Force Measurement

For a particular run, the value of drag force and hence the drag co-efficient was obtained by (ii) Measuring pressure at different angles around the periphery of the cylinder. The same procedure is repeated by varying diameter of the cylinder, free stream velocity and the roughness of the surface of the cylinder. In pressure distribution method, we used pressure coefficient, total pressure, static pressure, free stream velocity and angle of incidence.

3.4.2 Setup for the Pressure Distribution Experiments

- Fit the circular cylinder and protractor model into the first setup. Connect the model to the manometer .set the wind speed to maximum and the protractor to zero angle
- Record the surface pressure and static pressure. Rotate the protractor in 5^0 intervals for readings over the front half (0-90^0) then 10^0 intervals for readings over the rear half 90^0-180^0
- Monitor the total pressure and static pressure at the inlet to ensure that the wind speed is kept constant throughout the experiments.

Fig.3.5 Setup for Pressure Distribution method

3.5 EXPERIMENTAL CYLINDERS

The circular cylinder is built of 0.0480 m length, four different sizes of diameters i.e. 12.5 mm, 15mm, 20mm, and 25mm. For better information the details of geometrical parameters for both the experimental attachments are tabulated below and also Figure 3.6 (a, b) and Figure 3.7(a, b) shows details overview of smooth and rough surface cylinders.

Fig.3.6 (a) Used For Smooth Surface Cylinders with Varying Diameter

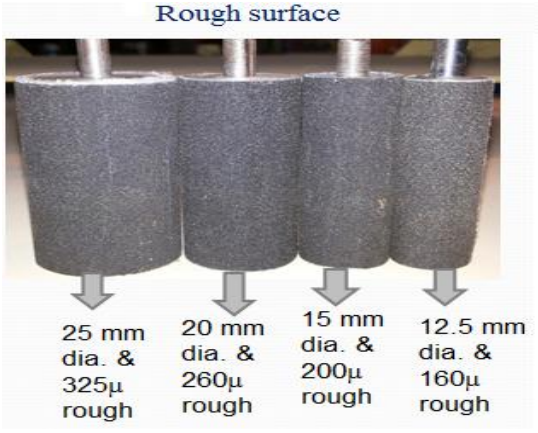

Fig.3.6 (b) Used For Rough Surface Cylinders with Different Roughness

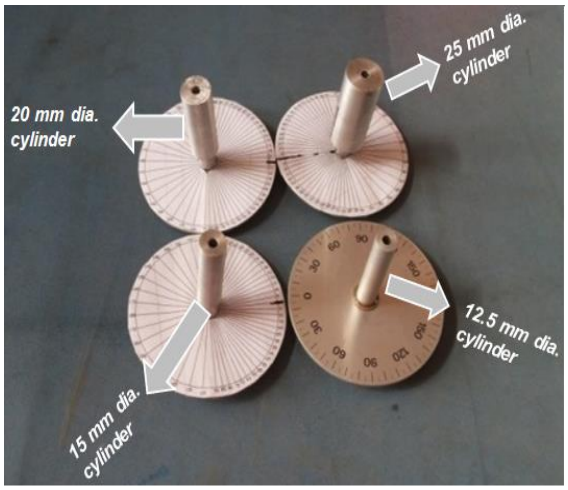

Fig.3.7 (a) Used For Smooth Surface Cylinders with Varying Diameter

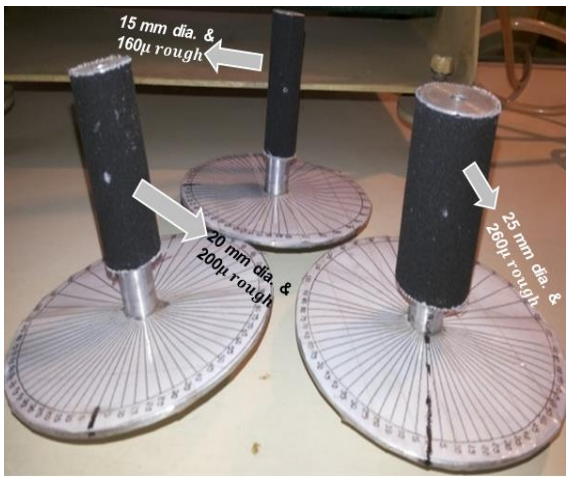

Fig.3.7 (b) Used For Rough Surface Cylinders with Different Roughness

Table 3.1: Details of Geometrical parameters of the experimental runs

Sl No	Item description	Present Experimental
1	Cylinder Type	Smooth and rough circular cylinder.
2	Cylinder size	12.5mm, 15mm, 20mm, 25mm diameter.
3	Cylinder length	0.048 m.
4	Air density	1.164 kg/m^3
5	Barometric pressure	1.04×10^5 n/m^2
6	Gas constant	287.2
7	Kinematic viscosity	1.6036×10^{-5} m^2/s
8	Roughness size	325micron,260micron,200micron,160micron

The detailed information on parameters of cylinder is provided in the table below.

Table 3.2 Scope of the experiment

DIRECT WEIGHING METHOD				PRESSURE DISTRIBUTION METHOD		
Diameter (mm)	Roughness (micron)	Velocity (m/s)		Diameter (mm)	Roughness (micron)	Velocity (m/s)
0.0125	325	8.26-26.14		0.015	325	26.50-23.41
	260	8.26-26.14			260	26.50-23.41
	200	8.26-26.14			200	26.50-23.41
	160	8.26-26.14			160	26.50-23.41
0.015	325	8.26-26.14		0.020	325	26.50-23.41
	260	8.26-26.14			260	26.50-23.41
	200	8.26-26.14			200	26.50-23.41
	160	8.26-26.14			160	26.50-23.41
0.020	325	8.26-26.14		0.025	325	26.50-23.41
	260	8.26-26.14			260	26.50-23.41
	200	8.26-26.14			200	26.50-23.41
	160	8.26-26.14			160	26.50-23.41
0.025	325	8.26-26.14		0.0125	smooth surface	26.50-23.41
	260	8.26-26.14				26.50-23.41
	200	8.26-26.14				26.50-23.41
	160	8.26-26.14				26.50-23.41

3.6 METHODOLOGY

The resistance of a body as it moves through a fluid is of great technical importance in hydrodynamics and aerodynamics. In this experiment we place a circular cylinder in an airstream and measure its resistance, or drag by two methods.

- Drag force by direct weighing method.
- Drag coefficient by pressure distribution method.

3.6.1 Drag Force by Direct Weighing Method

In the present context the word cylinder is used to describe a body which is generated by a straight line moving round a plane closed curve, its direction being always normal to the plane of a curve.

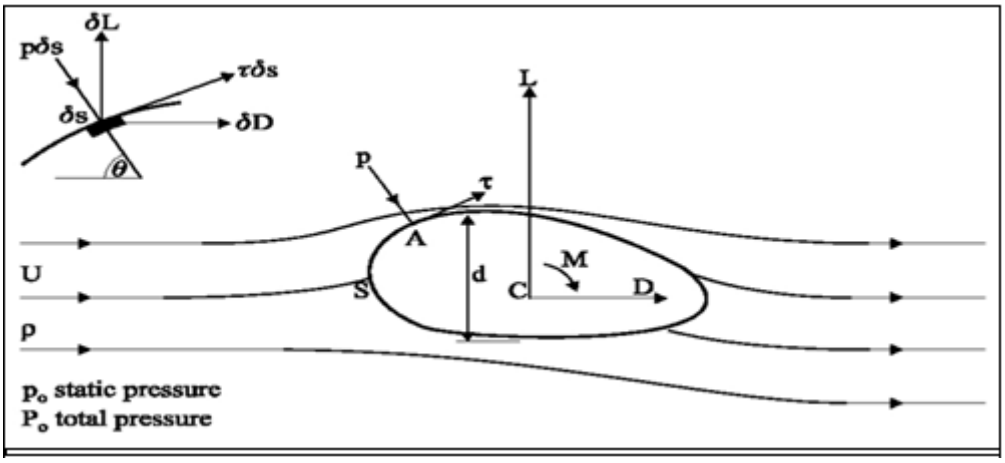

Fig.3.8 Cross section of a cylindrical body

An essential property of a cylinder is that its geometry is two-dimensional; each cross-section is exactly the same as every other cross-section, so that its shape may be described without reference to the dimension along the cylinder axis. Motion of the cylinder through stationary fluid produces actions on its surface which gives rise to a resultant force. From the point of view of an observer is moving with the cylinder, to which the fluid appears to be approaching

as a uniform stream. At any chosen point A of the surface of the cylinder, the effect of the fluid may conveniently be resolved into two components, pressure p normal to the surface and shear stress τ along the surface. It is convenient to refer absolute pressure p_a to the datum of static pressure p_0 in the oncoming stream; p is then a gauge pressure,

i.e.

$$P = p_a - P_0 \tag{3.1}$$

Let U denote the uniform speed of the motion and ρ the density of the fluid, then the dynamic pressure in the undistributed stream, $\frac{1}{2}\rho U^2$ is

$$\frac{1}{2}\rho U^2 = P_0 - p_0 \tag{3.2}$$

Where P_0 is total pressure

In this method we calculate the drag coefficient. We record the value of the drag force, total pressure, static pressure, dynamic pressure.

$$C_D = \frac{D}{\frac{1}{2}\rho U^2} \tag{3.3}$$

Where C_d= Drag coefficient

D= Drag Force

ρ = Air Density

U=Speed

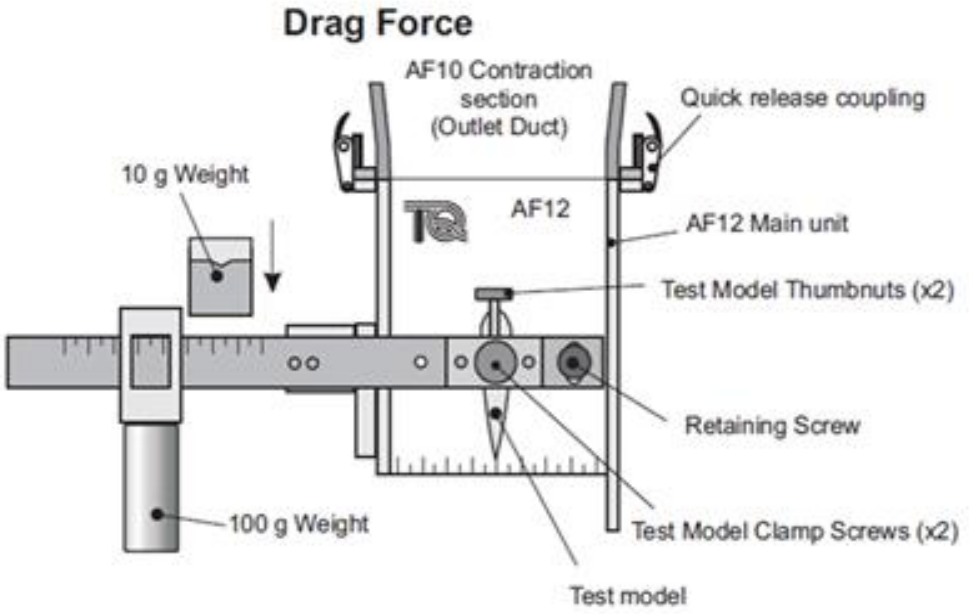

Fig.3.9 Apparatus diagram for Direct Weighing Method

3.6.2 Drag coefficient by pressure distribution Method

We know those pressure and skin friction coefficients are related to lift and drag. Consider an element of length δs of the surface, at a point where the normal is inclined at angle θ to the direction of U, as in Figure. (3.7)

The drag of a cylinder found by measuring p and τ over the surface and calculating the drag coefficient by equation (3.2)

$$C_D = \frac{1}{d} \oint \left(c_p \cos\theta + c_f \sin\theta \right) ds \qquad (3.4)$$

Now it is easy to measure the distribution of pressure over a cylinder but measurement of τ is a much more difficult task. The case of the circular cylinder, the contribution to drag from shear stress is found to be very much smaller than from pressure and may be neglected.

$$\delta s = R\delta\theta = \frac{d}{2}\,\delta\theta \qquad (3.5)$$

For the circular cylinder

$$C_D = \frac{1}{d} \oint c_p \cos\theta \left(\frac{d}{2}\right) d\theta \tag{3.6}$$

$$\therefore \qquad C_D = \frac{1}{d} \oint_0^{2\pi} c_p \cos\theta d\theta \tag{3.7}$$

For consideration of symmetry, we have

$$C_D = \oint_0^{2\pi} c_p \cos\theta d\theta \tag{3.8}$$

In this method we calculate drag coefficient. We record the value of the surface pressure, static pressure, total pressure& Pressure coefficient also.

$$C_P = \frac{P - p_0}{\frac{1}{2}\rho U^2} \tag{3.9}$$

Where C_P = pressure coefficient

P = surface pressure

P_0 = static pressure

ρ = air density

U= speed

Then

$$C_d = \int_0^{2\pi} C_p \cos\theta \tag{3.10}$$

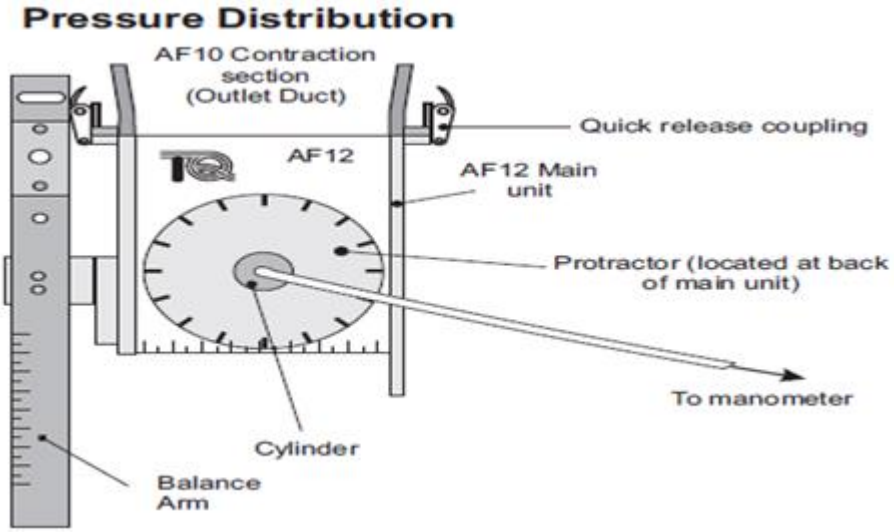

Fig.3.10 Apparatus diagram for Pressure Distribution Method

3.7 MEASUREMENT OF PRESSURE COEFFICIENT

The pressure coefficient is used in aerodynamics and hydrodynamics. The pressure coefficient is a dimensionless number which defines the relative pressures during a flow field in fluid dynamics. It is defined as the ratio of gauge pressure and dynamic pressure. Gauge pressure means total pressure minus static pressure.

3.8 MEASUREMENT OF DRAG COEFFICIENT

Drag coefficient is a dimensionless number that depends on the shape of the body and its orientation relative to the fluid stream. In this method, we calculate drag coefficient by this formula,

$$C_D = \frac{F_D}{\frac{1}{2}\rho A V^2} \tag{3.11}$$

In another method, we calculate drag coefficient by area under the curve, which is $c_p \cos\theta$ vs. angle of incidence.

CHAPTER IV
EXPERIMENTAL RESULTS

4.1 OVERVIEW

The results of experiments about the drag force, drag coefficient and pressure distribution in the Cylinders are presented in this chapter. Analysis is also done for drag coefficient of cylindrical bodies. The overall summary of experimental runs for the drag coefficient and pressure distribution.

This chapter will now present the results of these tests in terms of the drag force, drag coefficient and pressure distribution of the cylindrical bodies.

4.2 DRAG FORCE RESULTS

In direct weighing measurement method, variation of drag force in different parameters, such as velocity, diameter and roughness. Drag coefficient is inversely proportional to drag force. Variations of drag force with free stream velocity for the cylinders of varying roughness. Similarly the variation of drag force with velocity for the same roughness of cylinders of different diameters. The experimental data of drag force obtained under varying conditions of flow velocity and constant diameter of the cylinder. In this case diameter is constant, velocity increase and drag force increase. In smooth surface drag force is less when roughness increases drag forces will increases.

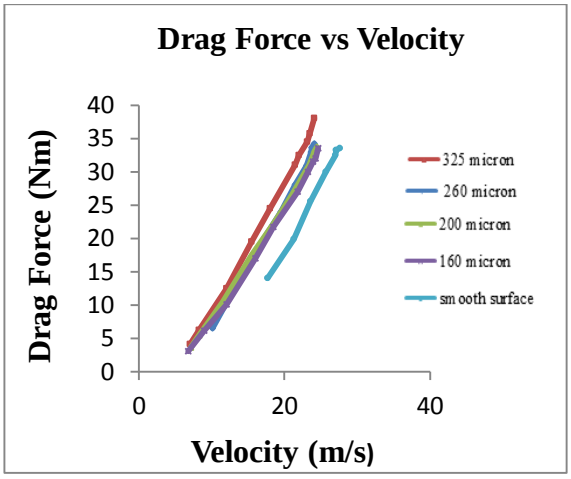

Fig.4.1 (i)

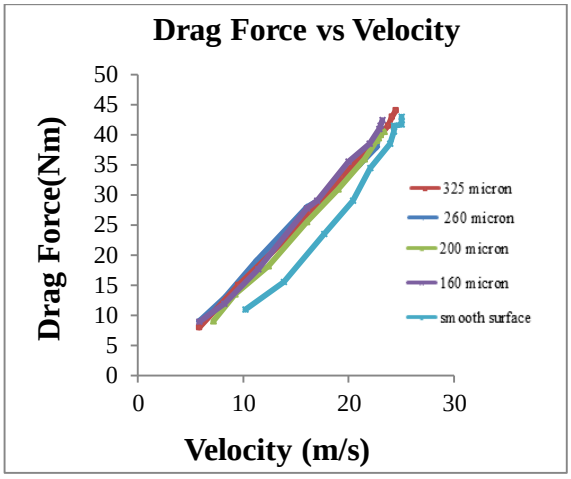

Fig.4.1 (ii)

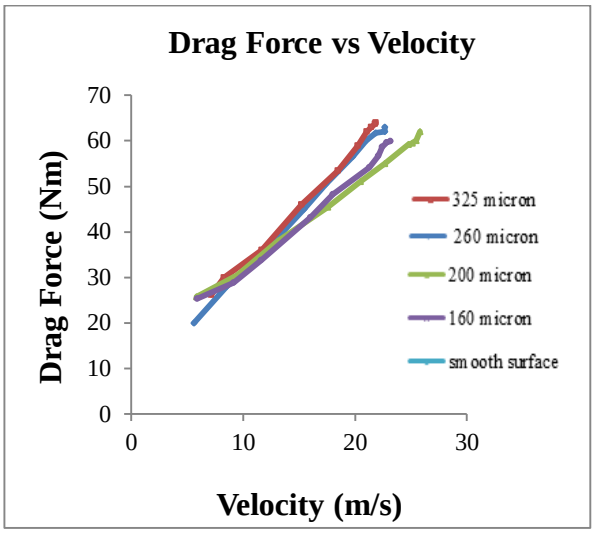

Fig.4.1 (iii)

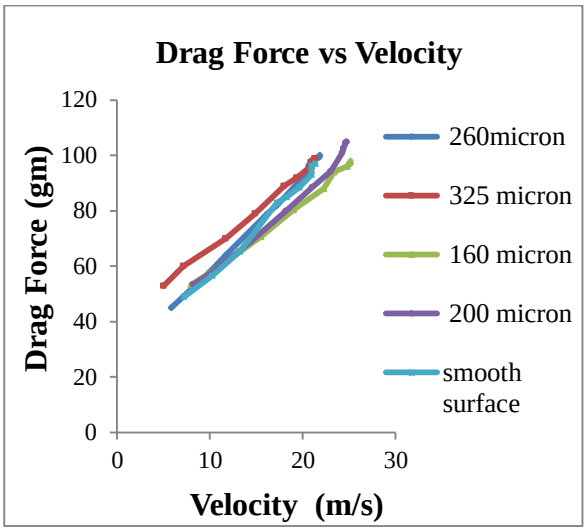

Fig.4.1 (iv)

Fig.4.1 (i)-Fig.4.1 (iv) Comparison between smooth and rough surface for 12.5mm, 15mm, 20mm and 25mm diameter

In Figure 4.1(I, ii, iii, iv) drag force vs velocity graphs are plotted for 12.5mm, 15mm, 20mm, 25mm diameter of cylinder by varying the roughness of the cylinder. From it is observed that with increase in roughness of the cylinder, the drag force is increasing with respect to the velocity.

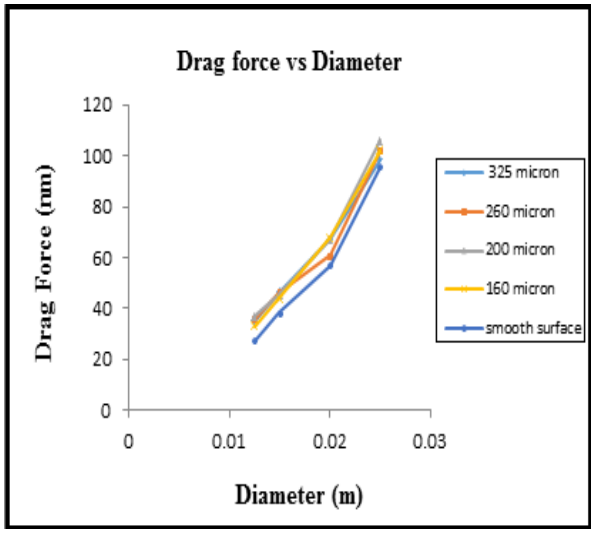

Fig.4.2 (i)

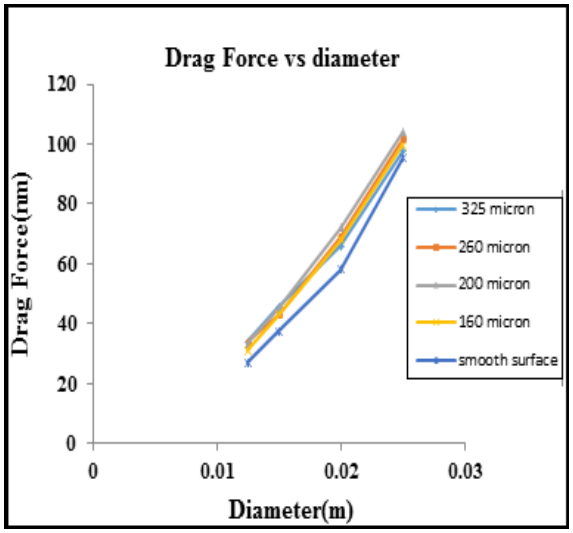

Fig.4.2 (ii)

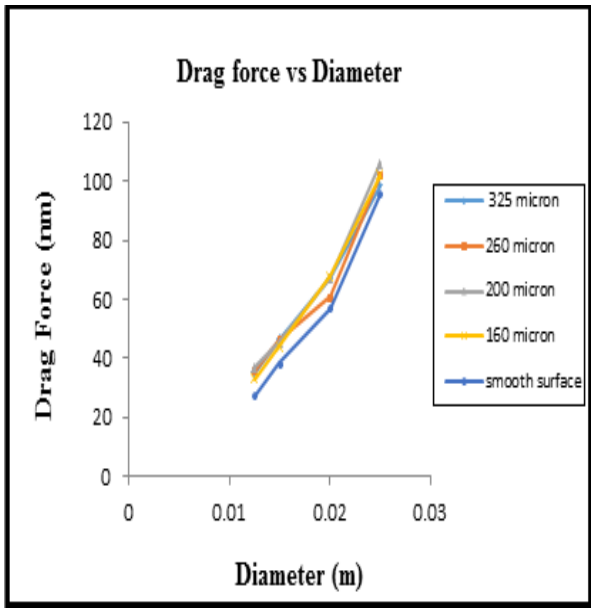

Fig.4.2 (iii)

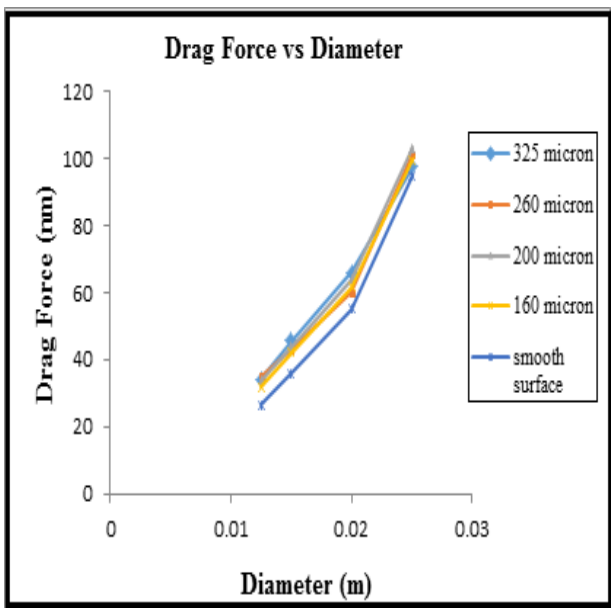

Fig.4.2 (iv)

Fig.4.2 (i)-Fig.4.2(iv) comparison between smooth and rough surface at constant velocity 26.14 m/s, 25.48m/s, 24.45m/s & 24.10m/s.

The four different graphs are plotted between the drag force and diameter of the cylinder for velocity of 26.14, 25.48, 24.45, 24.10 by varying roughness and smooth surface. From the graphs, it is found that the drag force is increasing with increase in roughness of the cylinder with respect to the diameter of the cylinder.

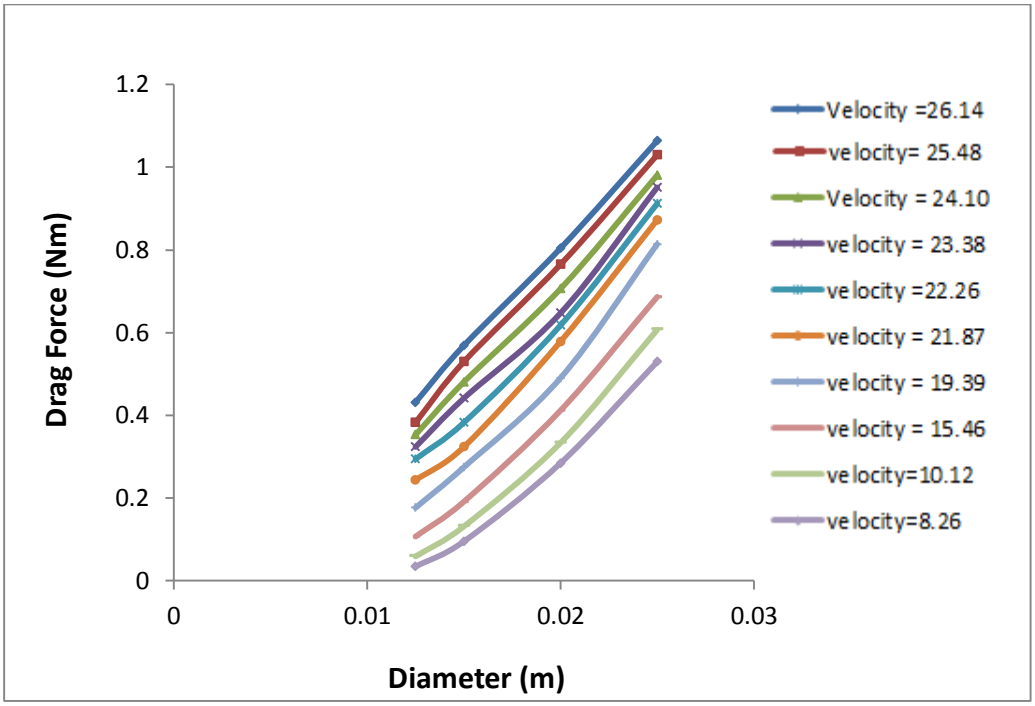

Fig.4.3 (i) Drag force vs. Diameter, comparison between in different velocity at constant roughness 326 micron

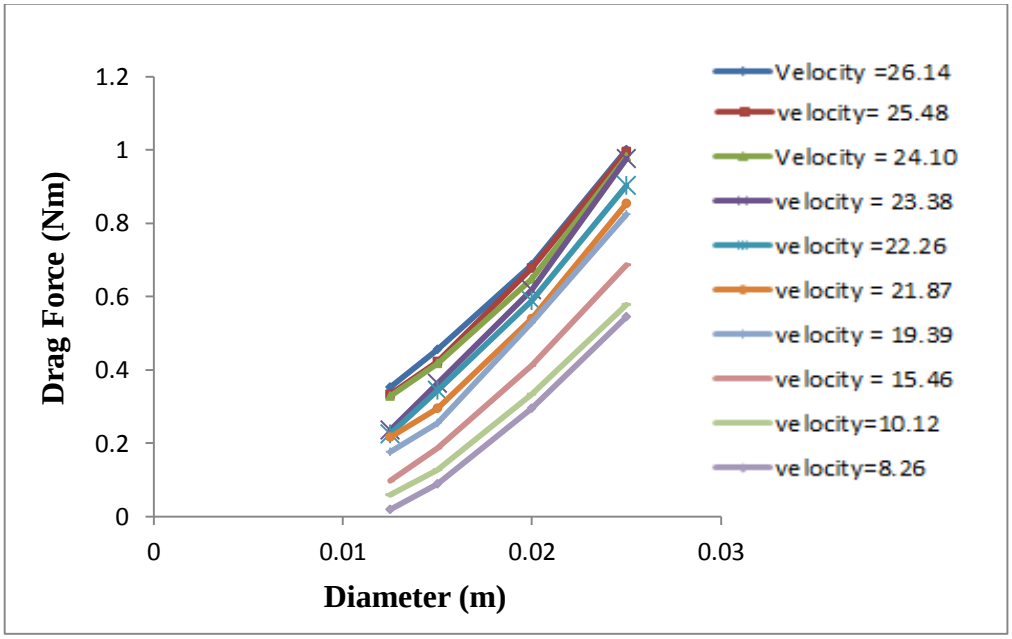

Fig.4.3 (ii) Drag force vs. Diameter, comparison between in different velocity at constant roughness 260 micron

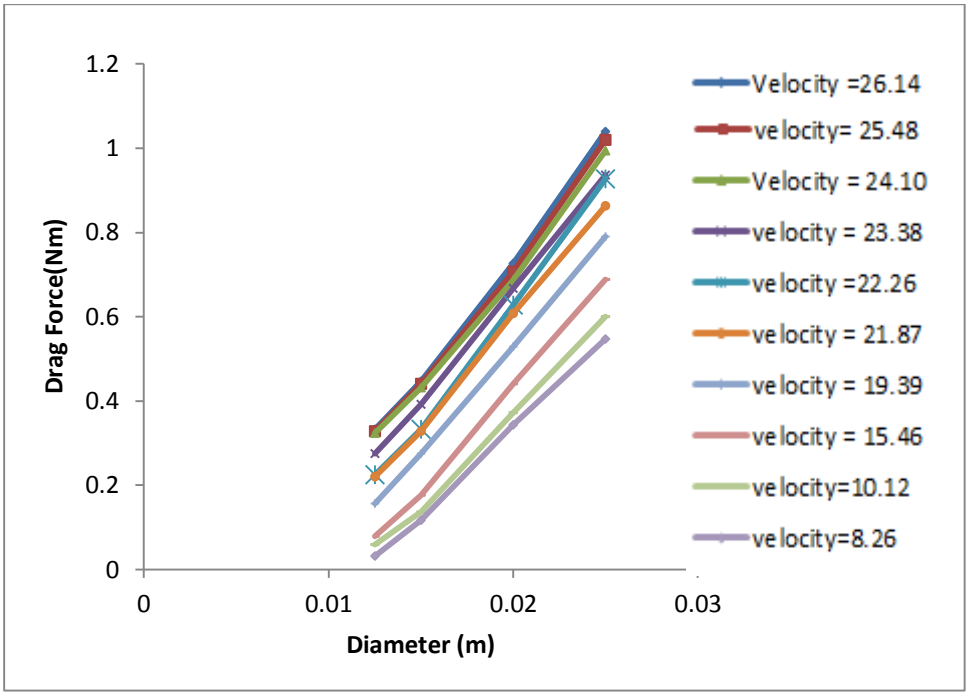

Fig.4.3 (iii) Drag force vs. Diameter, comparison between in different velocity at constant roughness 200 micron

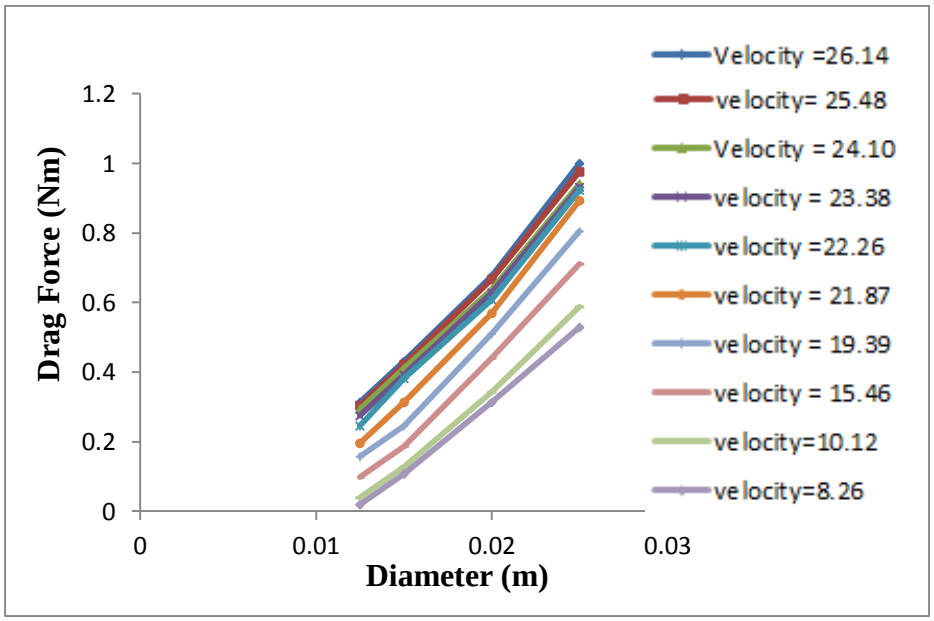

Fig.4.3 (iv) Drag force vs. Diameter, comparison between in different velocity at constant roughness 160 micron

From roughness 326, 260, 200 and 160 micron the above graph Fig.4.3 (I, ii, iii & iv) is plotted between the drag force and diameters of the cylinders by varying the velocity of airflow. From the graph it is found that the drag force is increasing with increase in velocity of the flow with respect to diameter of the cylinder.

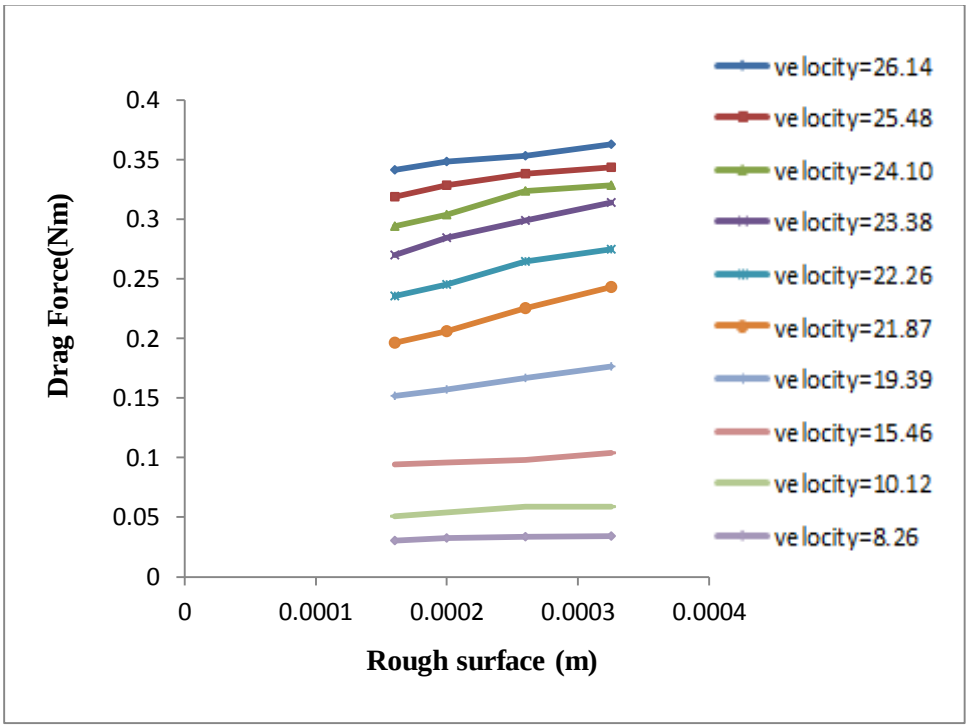

Fig.4.4 Comparison between Drag forces vs. Roughness, in different velocity at constant diameter

A graph is plotted between drag force vs roughness at a constant diameter of 12.5mm of the cylinder by varying the velocity of the flow. From the graph it is observed that with increase in velocity, the drag force is also increasing with respect to roughness.

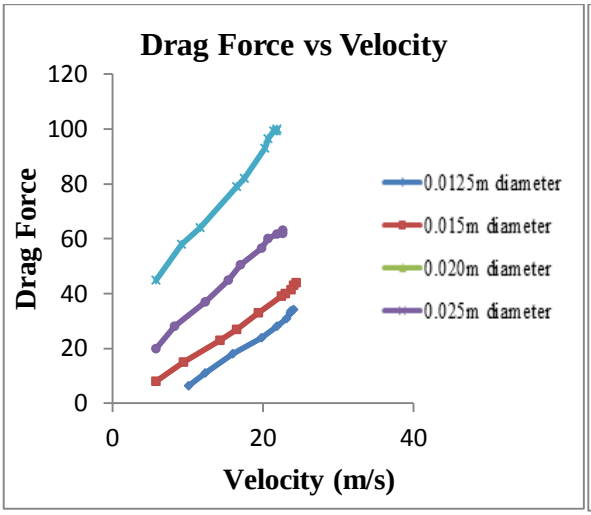

Fig.4.5 (i)

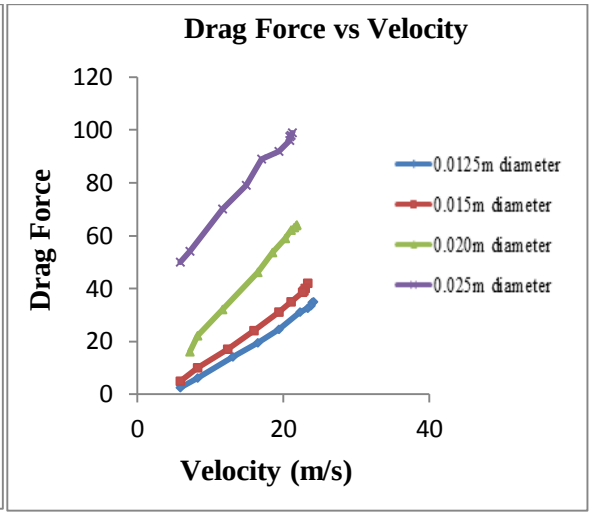

Fig.4.5 (ii)

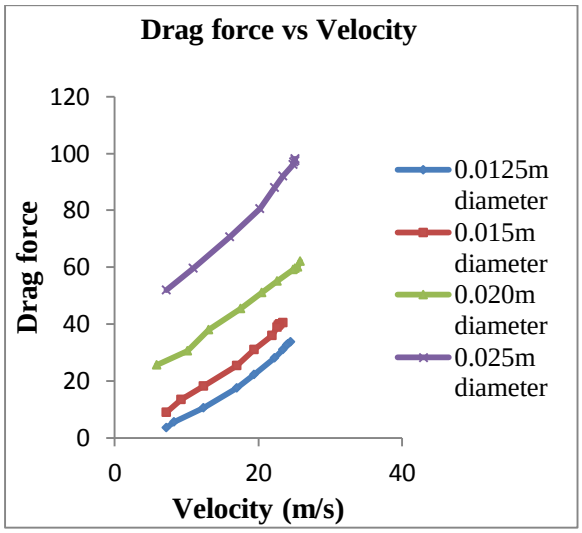

Fig.4.5 (iii)

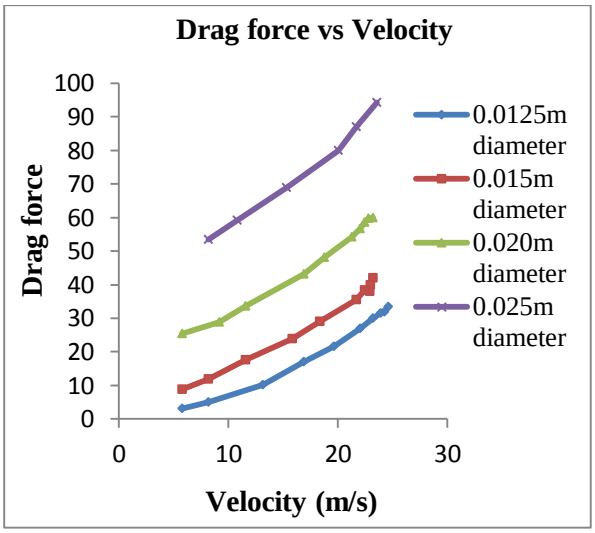

Fig.4.5 (iv).

Fig.4.5(i)-Fig.4.5(iv) Drag force vs.velocity, in different diameter at constant roughness 325 micron, 260micron, 200micron and 160micron

The graph is plotted between drag force vs velocity at a roughness of 325,260,200 & 160 micron by varying the diameter of the cylinder. From the graph it is found that with increase in the value of the roughness, the drag force is also increasing with respect to velocity.

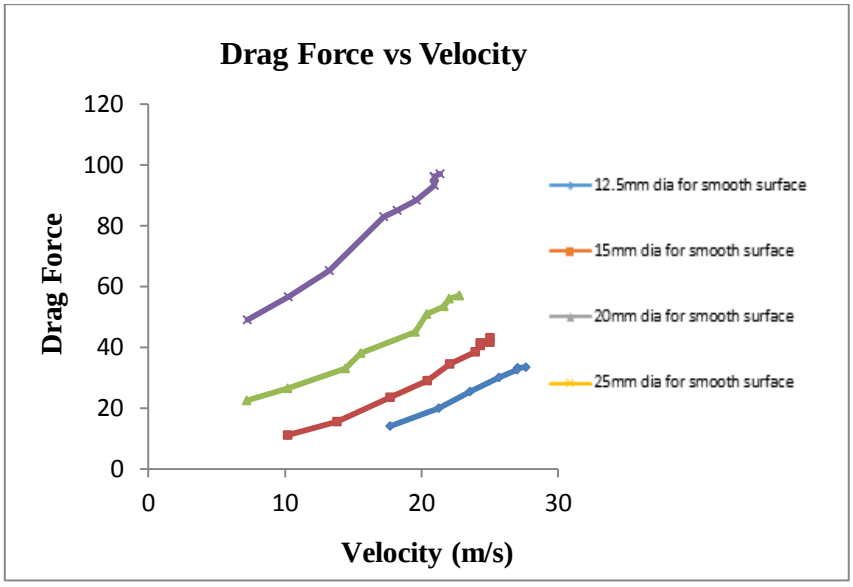

Fig.4.6 Drag force vs. velocity, in different diameter at smooth surface

The graph is plotted between drag force vs.velocity and the variation of drag force increase when the smooth surface of different diameter of cylinder is increase. Because the surface area is increased, so that the drag force is also increase.

4.3 PRESSURE DISTRIBUTION METHOD

In pressure distribution method, variation of pressure coefficient is occurred through different parameters such as velocity, diameter and roughness. Variations of pressure coefficient occur with free stream velocity for the cylinders of varying roughness. Similarly the variations of pressure coefficient occur with velocity for the same roughness of cylinders of different diameters. For pressure distribution at varying location for the cylinder of same roughness and varying diameters are considered. The experimental data of drag force obtained under varying conditions of flow velocity and constant diameter of the cylinder. In this case diameter is constant, velocity increase and drag force increase. In smooth surface drag force is less when roughness increases drag forces will increases.

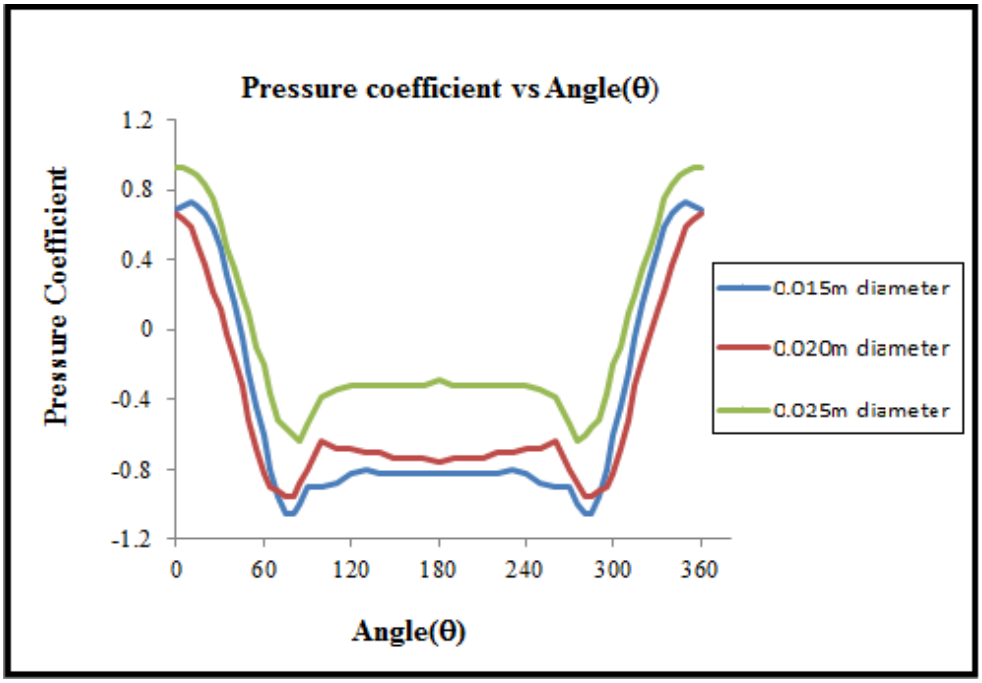

Fig. 4.7(i) Comparison 325 micron roughness of cylinder at constant Velocity=26.50 m/s

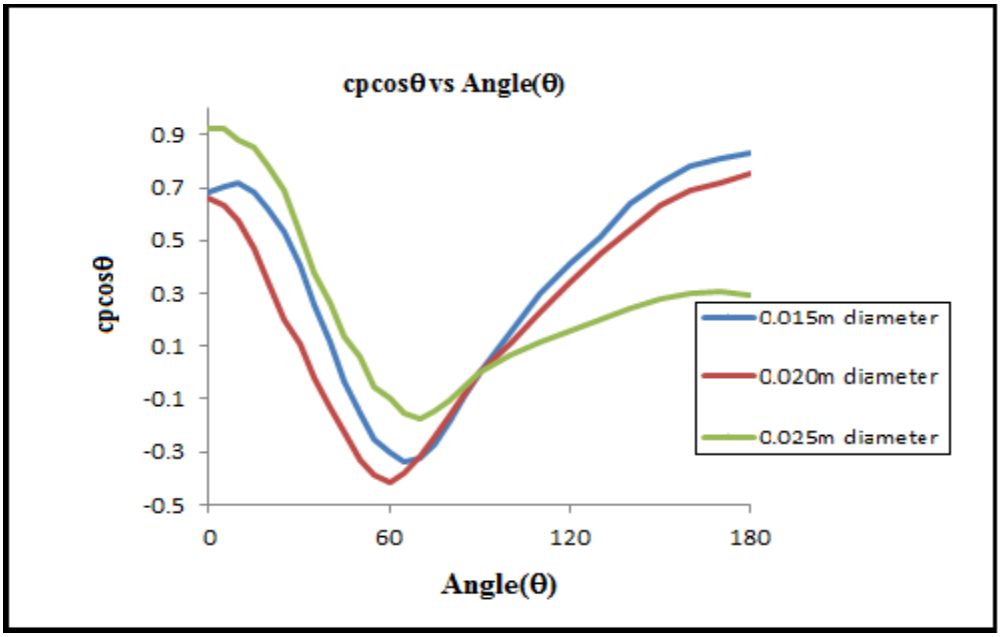

Fig.4.7 (ii) Comparison 325 micron roughness of cylinder at constant Velocity=26.50 m/s

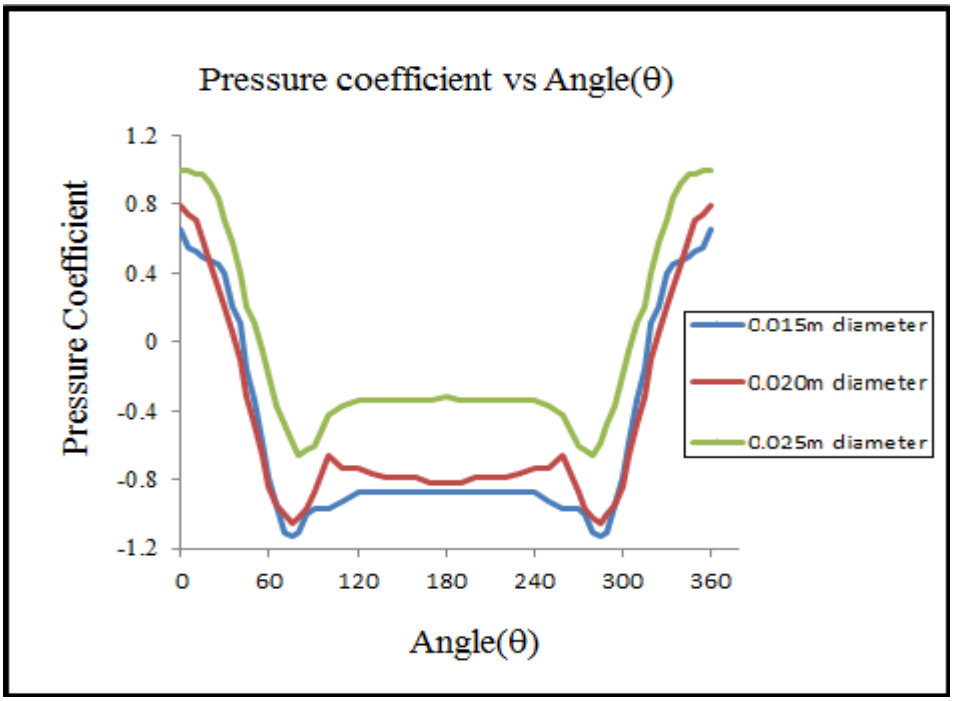

Fig.4.8 (i) Comparison 260 micron roughness of cylinder at constant Velocity=26.50m/s

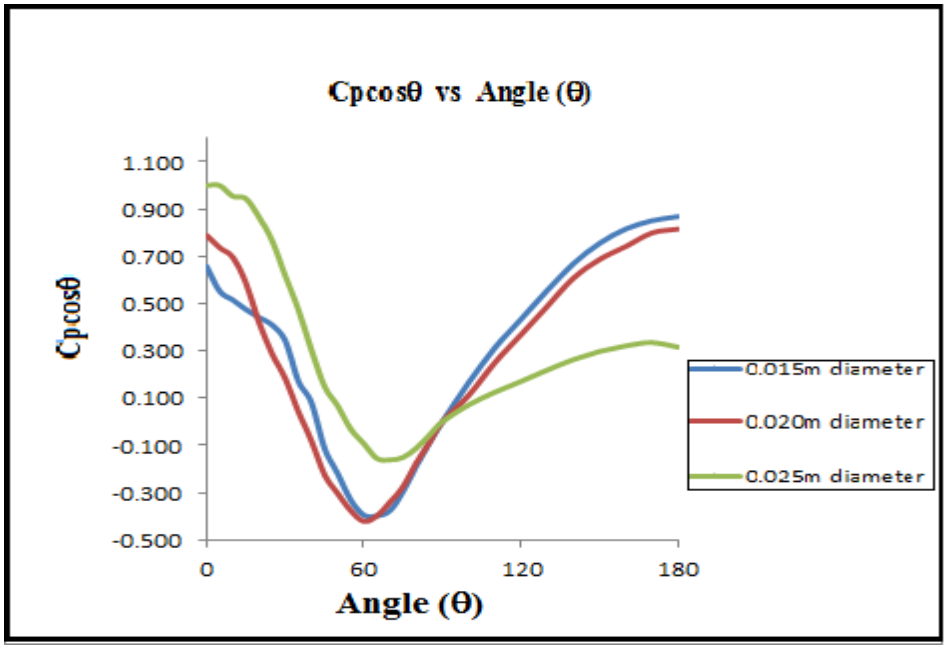

Fig.4.8 (ii) Comparison 260 micron roughness of cylinder at constant Velocity=26.50m/s

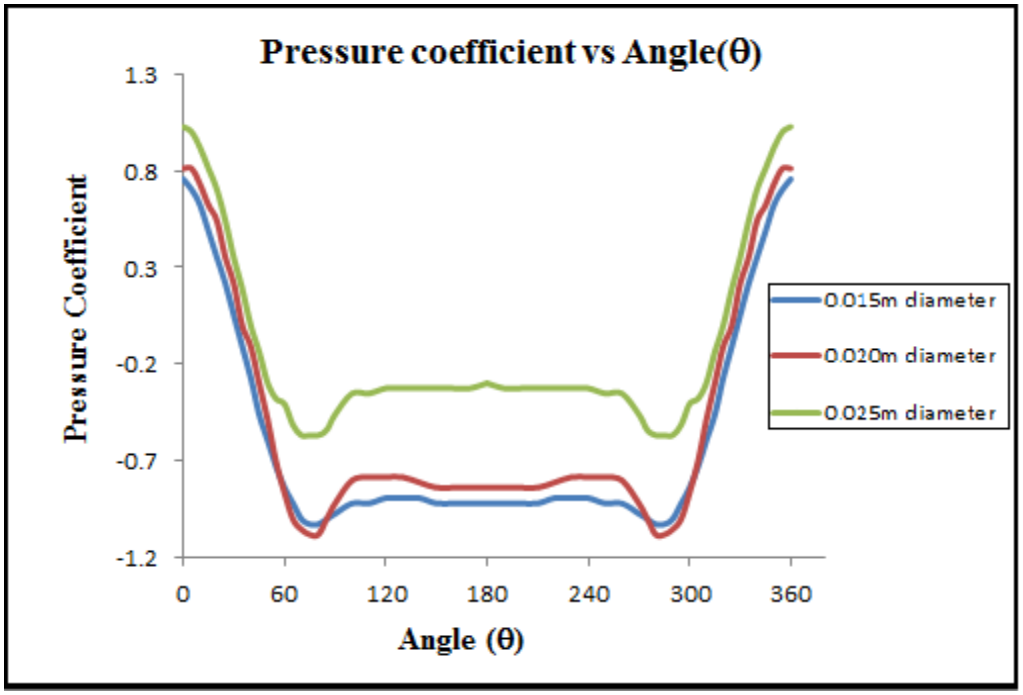

Fig.4.9 (i) Comparison 260 micron roughness of cylinder at constant Velocity=25.18m/s

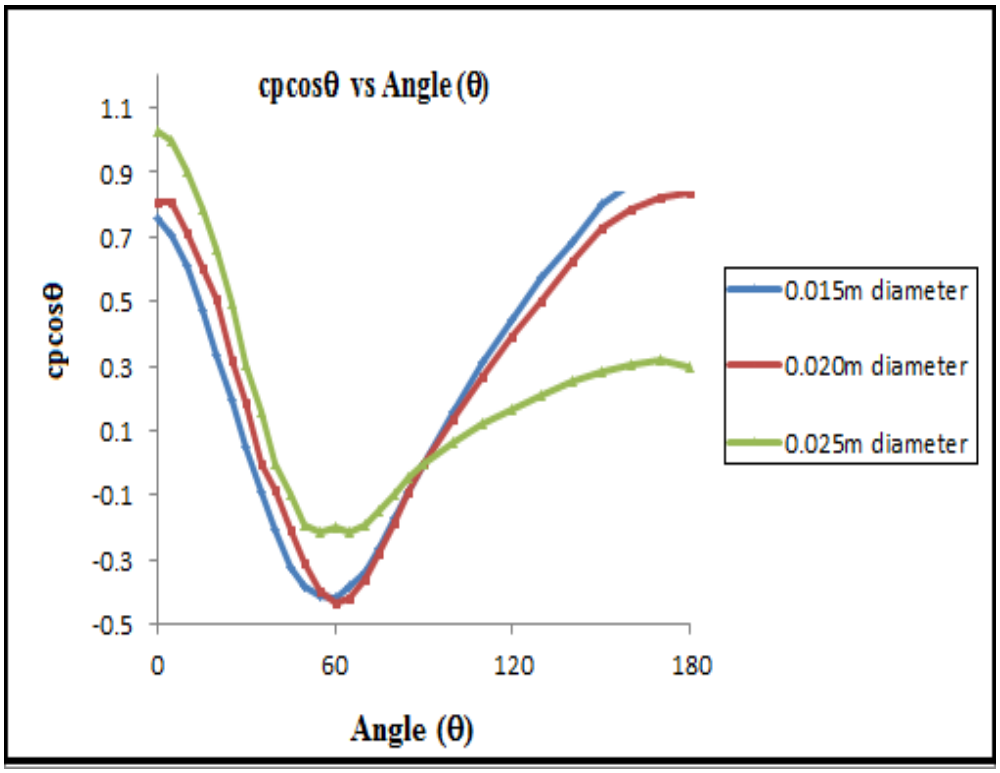

Fig.4.9 (ii) Comparison 260 micron roughness of cylinder at constant Velocity=25.18m/s

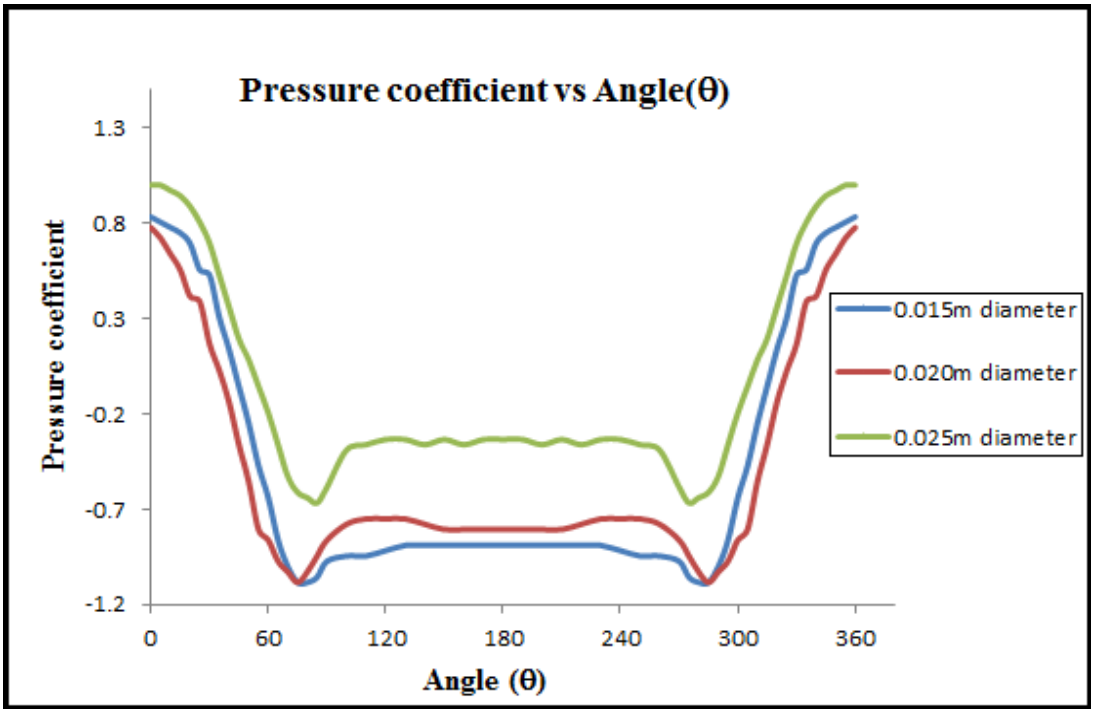

Fig.4.10 (i) Comparison 260 micron roughness of cylinder at constant Velocity=24.83m/s

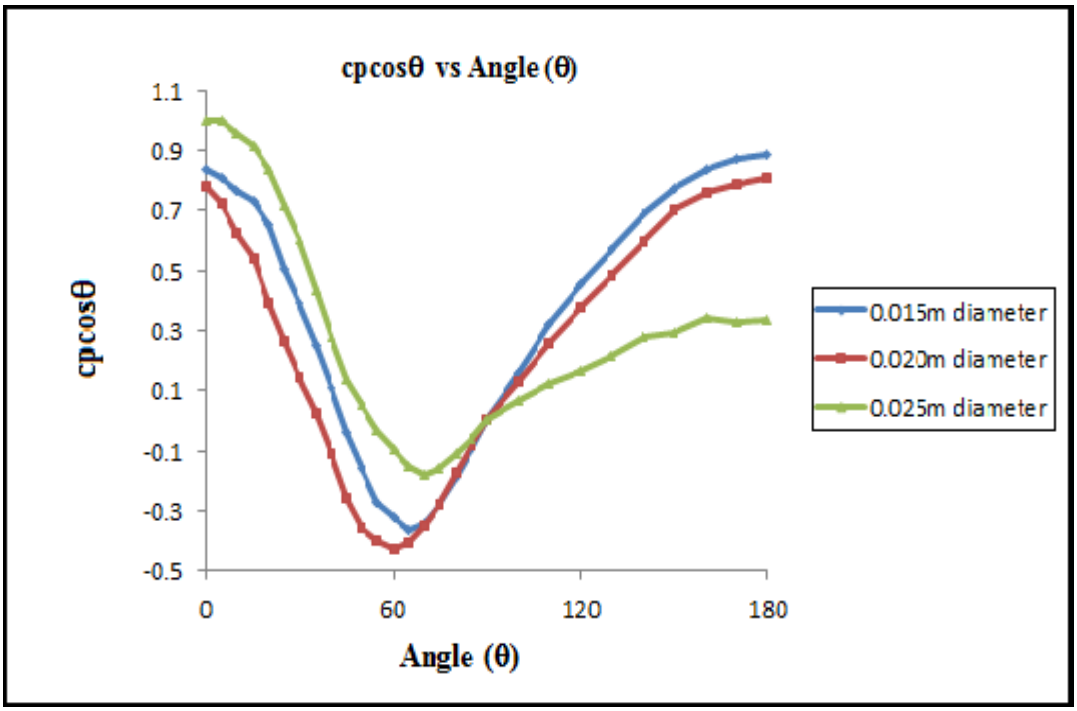

Fig.4.10 (ii) Comparison 260 micron roughness of cylinder at constant Velocity=24.83m/s

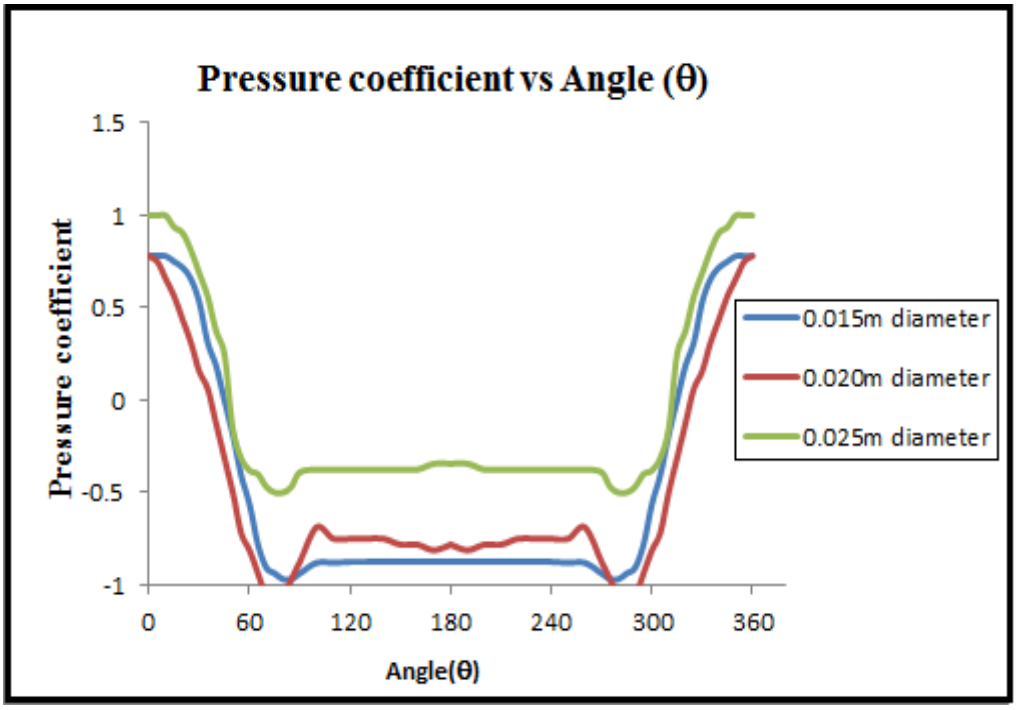

Fig.4.11 (i) Comparison 260 micron roughness of cylinder at constant Velocity=23.41m/s

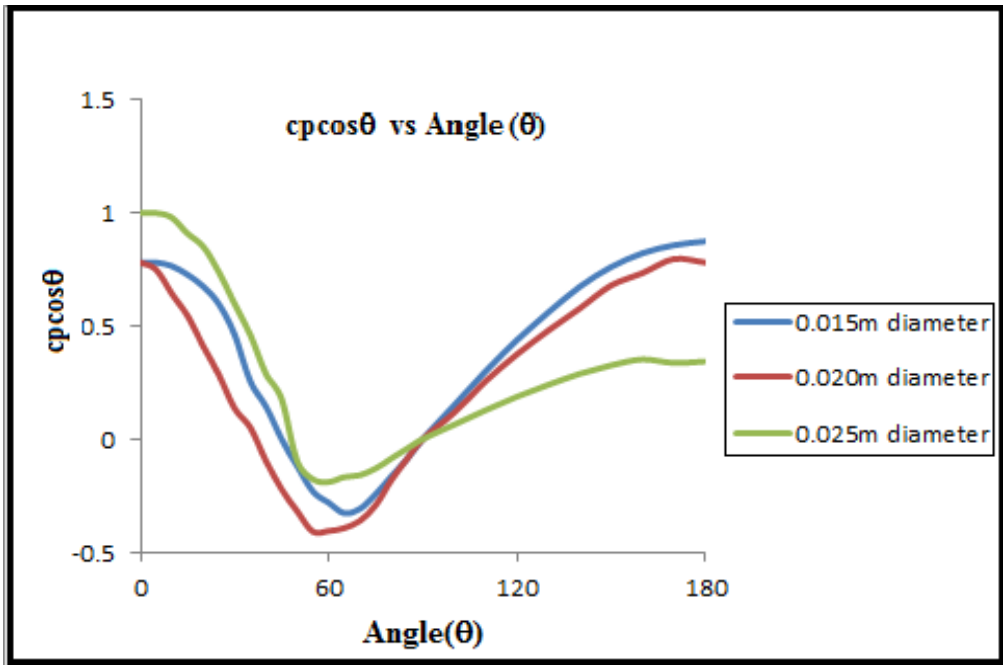

Fig.4.11 (ii) Comparison 260 micron roughness of cylinder at constant Velocity=23.41m/s

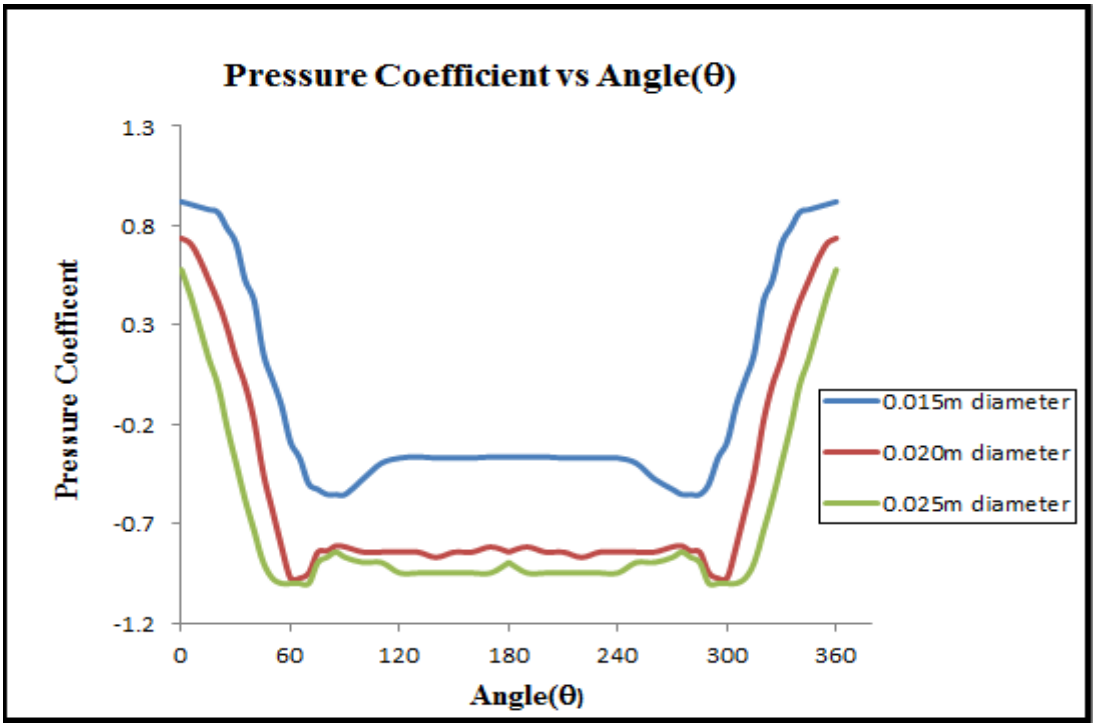

Fig.4.12 (i) Comparison 200 micron roughness of cylinder at constant Velocity=26.50m/s

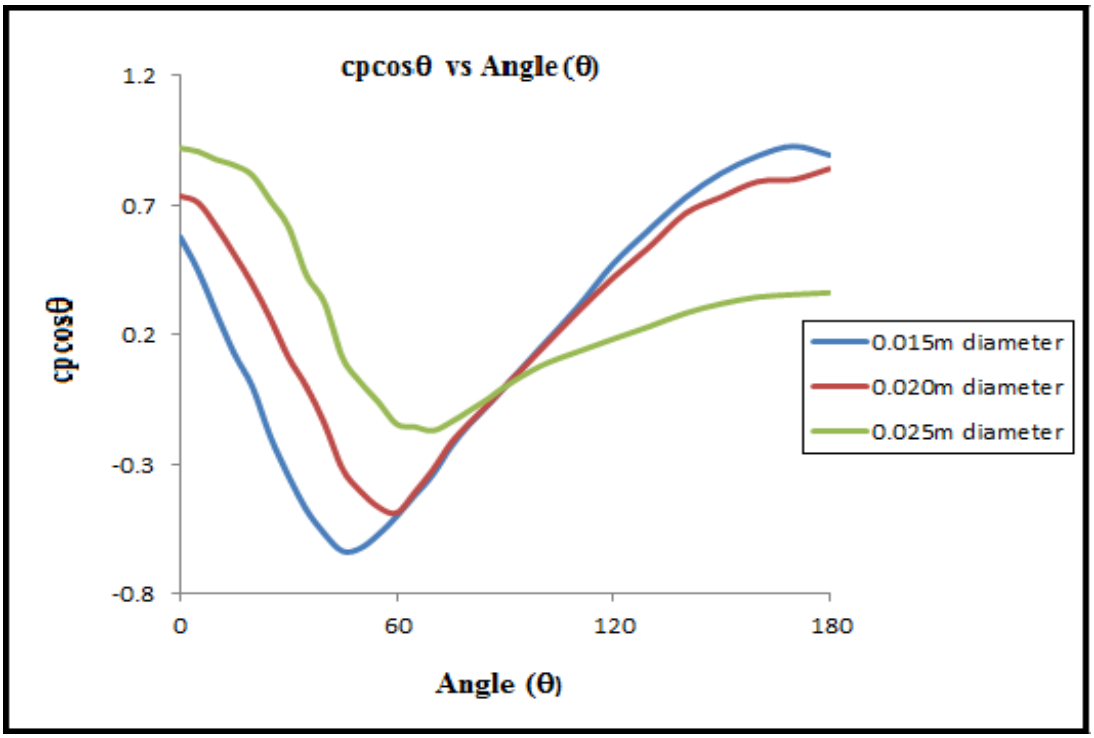

Fig.4.12 (ii) Comparison 200 micron roughness of cylinder at constant Velocity=26.50m/s

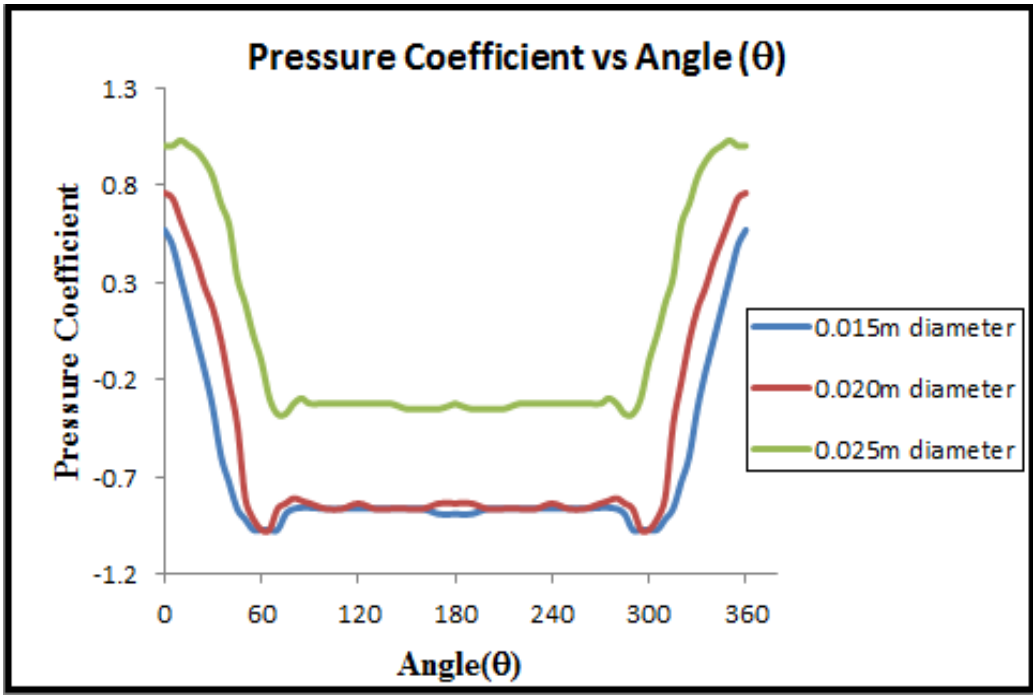

Fig.4.13 (i) Comparison 200 micron roughness of cylinder at constant Velocity=25.18m/s

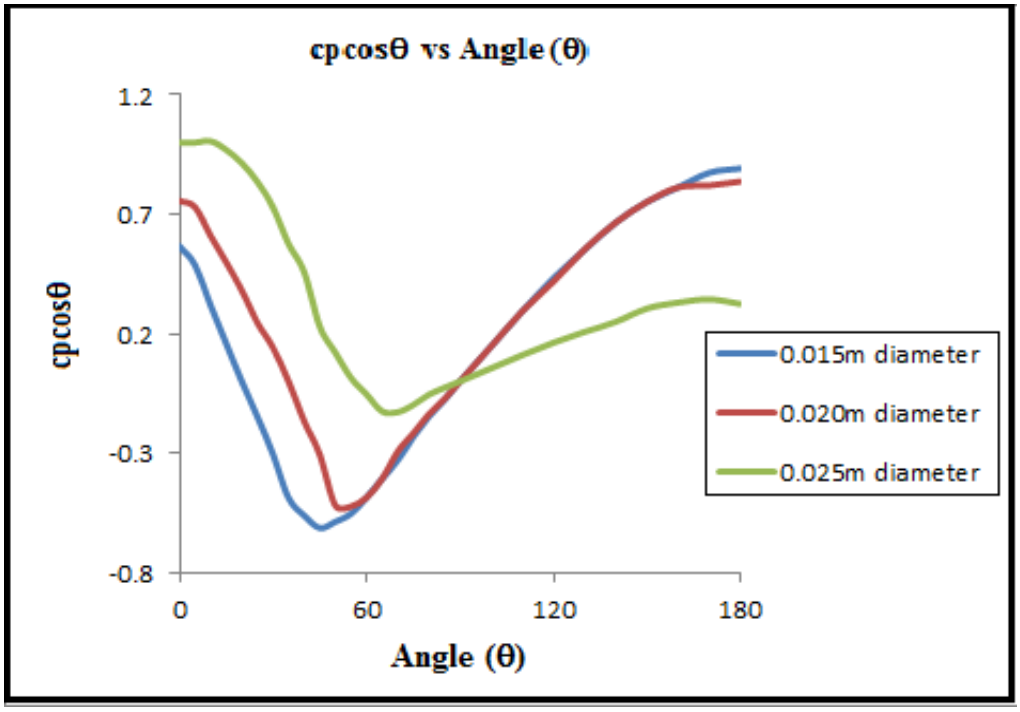

Fig.4.13 (ii) Comparison 200 micron roughness of cylinder at constant Velocity=25.18m/s

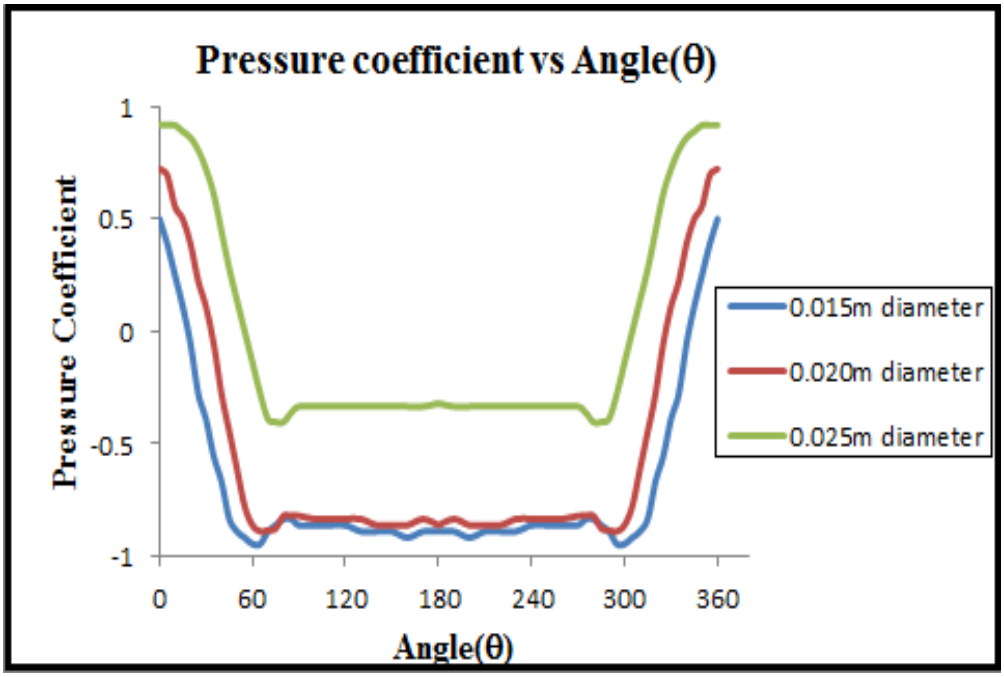

Fig.4.14 (i) Comparison 200 micron roughness of cylinder at constant Velocity=24.83m/s

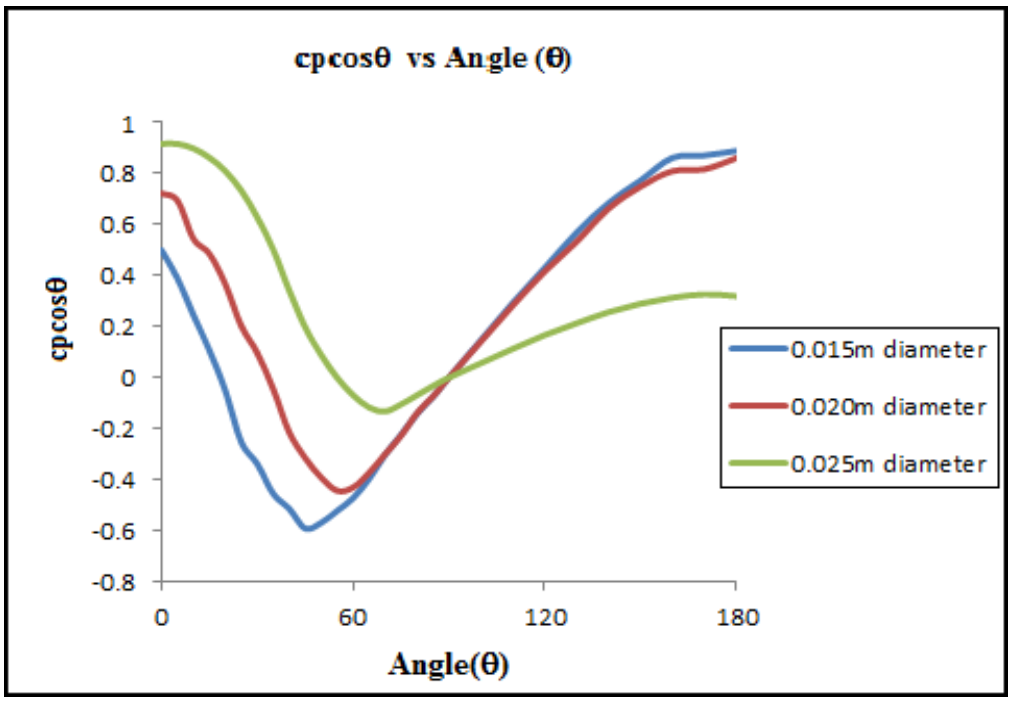

Fig.4.14 (ii) Comparison 200 micron roughness of cylinder at constant Velocity=24.83m/s

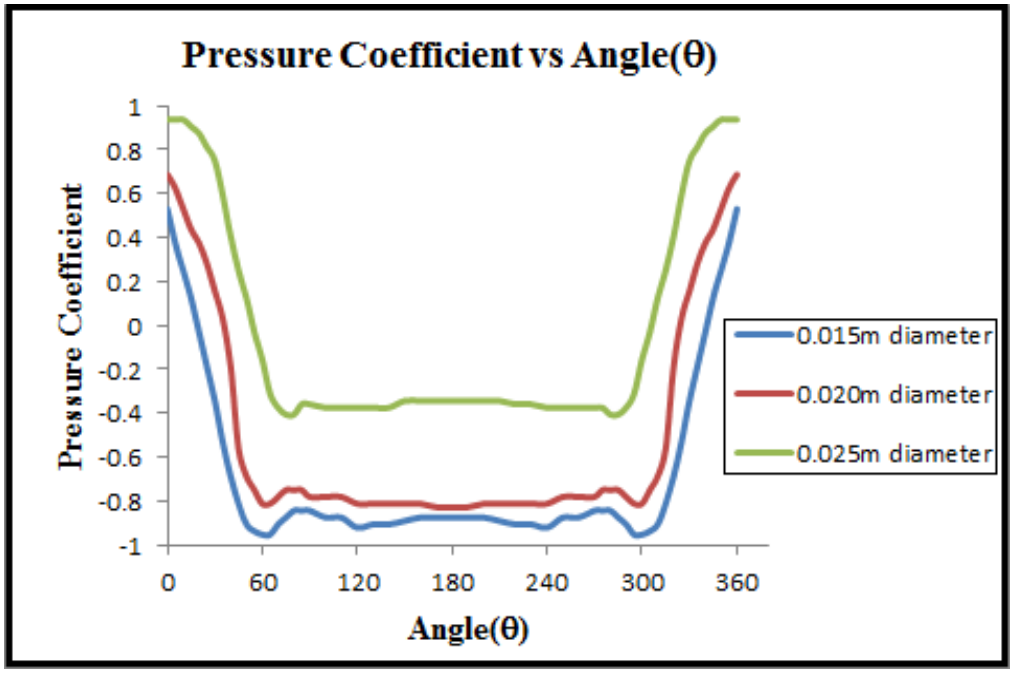

Fig.4.15 (i) Comparison 200 micron roughness of cylinder at constant Velocity=23.41m/s

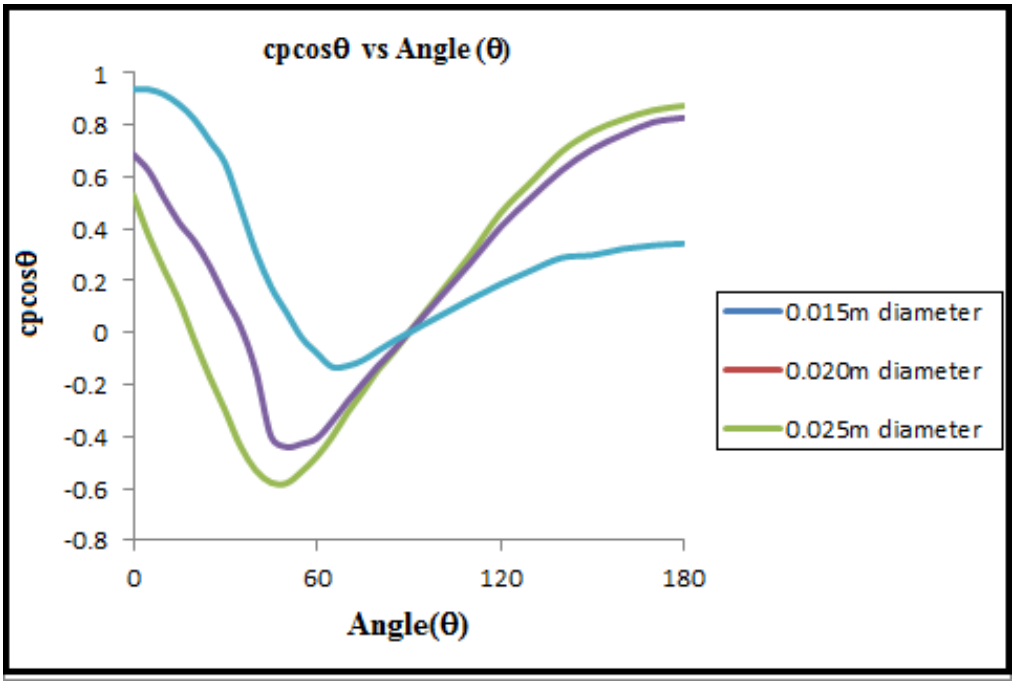

Fig.4.15 (ii) Comparison 200 micron roughness of cylinder at constant Velocity=23.41m/s

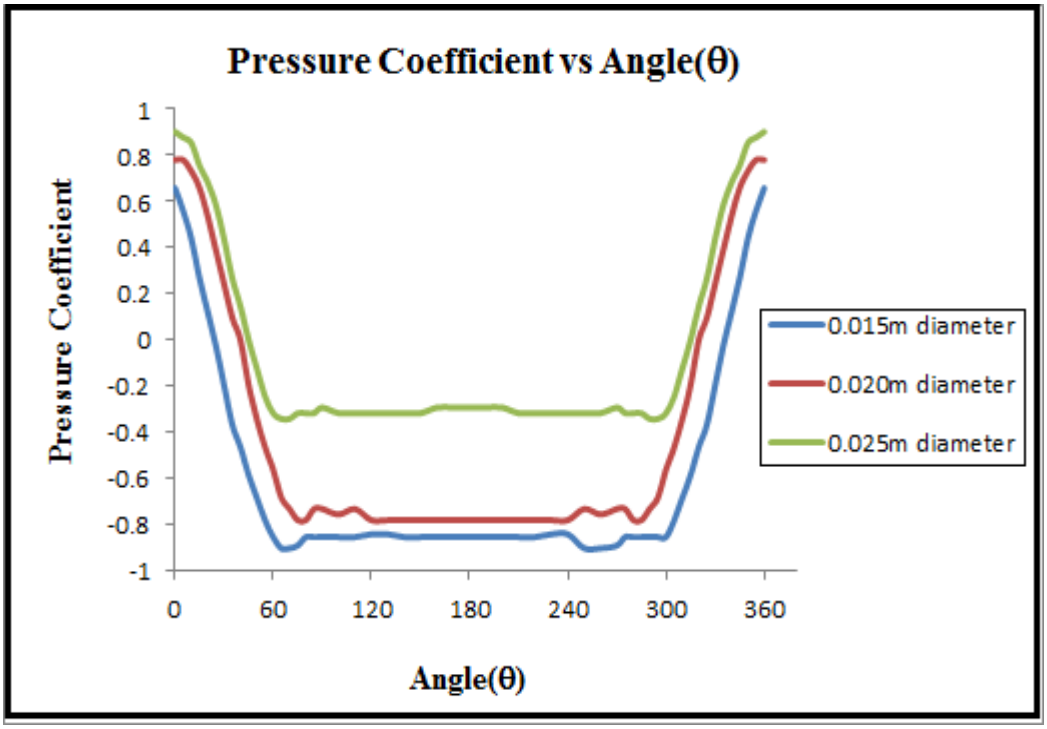

Fig.4.16 (i) Comparison 160 micron roughness of cylinder at constant Velocity=26.50m/s

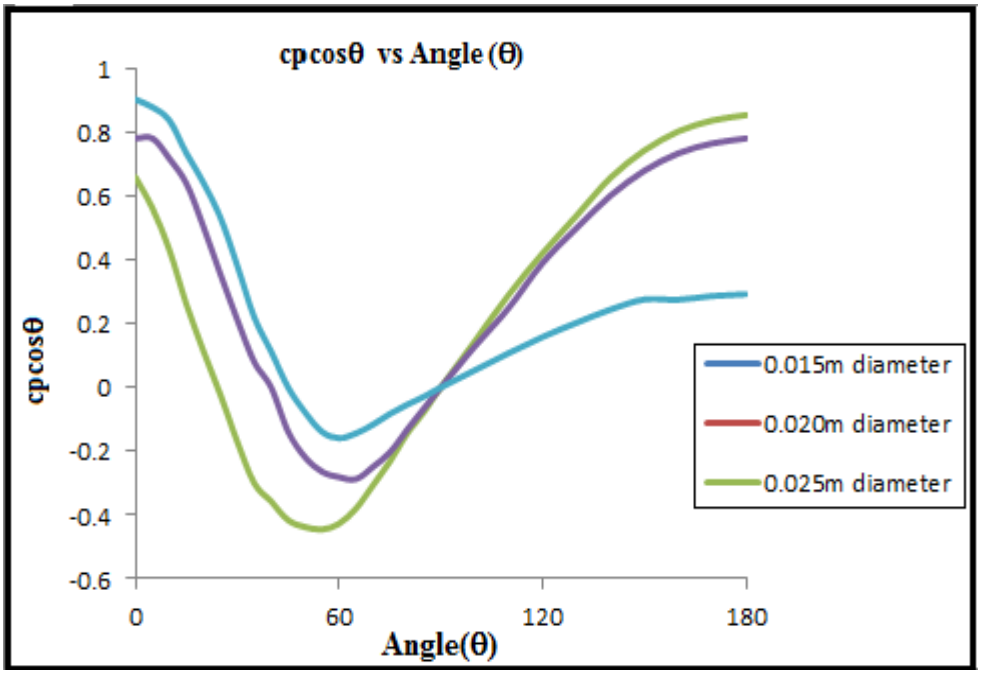

Fig.4.16 (ii) Comparison 160 micron roughness of cylinder at constant Velocity=26.50m/s

CHAPTER V
DIMENSIONAL AND MODEL ANALYSIS

5.1 OVERVIEW

The Rayleigh's method of dimensional analysis becomes more difficult if the variables are more than the number of fundamental dimensions (M, L, and T). This difficulty is overcome by using **Buckingham's π-theorem**, which states, "if there are n variables in a physical phenomenon and if these variables contain m fundamental dimensions (M, L, T), then the variables are arranged into m-n dimensionless terms. Each term is called **π-term**.

Let X_1, X_2, X_3….. X_n are the variables involved in a physical problem. Let X_1 be the **dependent variable** and X_2, X_3… X_n are the **independent variables** on which X_1 depends. Then X_1 is a function of X_2, X_3,….. X_n and mathematically it is expressed as

$$X_1 = f(X_2, X_3, \dots\dots\dots X_4) \tag{5.1}$$

Equation (5.1) can also written as

$$f_1(X_1, X_2, X_3, \dots\dots\dots X_n) = 0 \tag{5.2}$$

Equation (5.2) is a dimensionally **homogenous equation**. It contains n variables. According to **Buckingham π- theorem**, the number of dimensionless group or π-terms in which number of π-terms is equal to (n-m).

Hence

$$f(\pi_1, \pi_2, \dots\dots\pi_{n-m}) = 0 \tag{5.3}$$

Each π-terms is dimensionless and is independent of the system of unit. Each π-term contains m+1 variables, where m is the number of fundamental dimensions required to describe the variables completely. From the variables listed for the phenomena, three variable

one each from **linear dimension**, **flow properties** and **fluid properties** are chosen as repeating variable. If X_2, X_3 and X_4 are selected for repeating variables, then each π- term is written as

$$\left.\begin{aligned}\pi_1 &= X_2^{a1}.X_3^{b1}.X_4^{c1}.X_1\\ \pi_2 &= X_2^{a2}.X_3^{b2}.X_4^{c2}.X_5\\ \pi_{n-m} &= X_2^{a_{n-m}}.X_3^{b_{n-m}}.X_4^{c_{n-m}}.X_n\end{aligned}\right\} \quad (5.4)$$

Each equation is solved by the principle of dimensional homogeneity and values of exponents a_1, b_1, c_1 etc., are obtained. These values are substituted in above equation (5.4) to get of π_1, π_2, π_{n-m} and subsequently put in equation (5.3).

5.2 CORRELATION OF DIMENSIONLESS FORM

The drag force F_D is a function of V, D,ρ,μ, k

Mathematically,

$$F_D = f(V, D, \rho, \mu, k,) \quad (5.5)$$

The above equation can also be written as under:

$$f(F_D, V, D, \rho, \mu, k) = 0 \quad (5.6)$$

Where n = No. of total variables involved in the phenomena = 6

m =3, no. of fundamental quantity required to describe all the variables

No. of π terms = 6-3 = 3

Now, choosing V, D, ρ as repeating variables, each π-term can be expressed as under:

$$\pi_1 = V^{a1}D^{b1}\rho^{c1}\mu \quad (5.7)$$

$$\pi_2 = V^{a2} D^{b2} \rho^{c2} k \quad (5.8)$$

$$\pi_3 = V^{a3} D^{b3} \rho^{c3} F_D \quad (5.9)$$

Dimensions of each variable are:

V=$[M^0 L^1 T^{-1}]$, (5.10)

D=$[M^0 L^1 T^0]$, (5.11)

ρ =$[M^1 L^{-3} T^0]$, (5.12)

$k = [M^0 L^1 T^0]$, (5.13)

μ =$[M^1 L^{-1} T^{-1}]$, (5.14)

$F_D = [M^1 L^1 T^{-2}]$ (5.15)

Thus three π-terms sayπ_1,π_2, and π_3 are formed.

$f_1(\pi_1 \pi_2 \pi_3) = 0$ (5.16)

each π-term = m+1 variables, where m is equal to 3 and also called repeating variables. Out of six variables$F_D, V, D, \rho, \mu, and\ k$, three variables are to be selected as repeating variable. $F_D$is a dependent variable and should not be selected as a repeating variable. Out of the five remaining variables. One variable should have flow property; the second variable should have geometric property and third one fluid property. These requirements are fulfilled by selecting V, D and ρ as repeating variables. The repeating variables themselves should not form a dimensionless term and should have themselves fundamental dimensions equal to m, i.e. 3 here. Dimension of V, D and ρ are V=$[M^0 L^1 T^{-1}]$, D=$[M^0 L^1 T^0]$, and ρ =$[M^1 L^{-3} T^0]$ and hence the three fundamental dimensions exist in V, D and ρ and they themselves do not form dimensionless group.

Each π-term is written as according to equation (5.5)

Each π-term is solved by the principle of dimensional homogeneity. For the first π-term, we have

$$\pi_1 = V^{a1} D^{b1} \rho^{c1} \mu$$

$$[M^0 L^0 T^0] = [M^0 L^1 T^{-1}]^{a1} . [M^0 L^1 T^0]^{b1} [M^1 L^{-3} T^0]^{c1} [M^1 L^{-1} T^{-1}]$$

Equating the powers of M, L, and T on both sides, we get

Power of M, c_1= (-1)

Power of L, a_1 = (-1)

Power of T, b_1 = (-1)

Substituting the values of a_1, b_1 and c_1 in equation (5.5)

π_1= $(V)^{-1}(D)^{-1}(\rho)^{-1}\mu$

$$\pi_1 = \frac{\mu}{\rho V D} = R_e$$

Similarly for the second π-term, we get

$$\pi_2 = V^{a2} D^{b2} \rho^{c2} k$$

$$[M^0 L^0 T^0] = [M^0 L^1 T^{-1}]^{a2} . [M^0 L^1 T^0]^{b2} [M^1 L^{-3} T^0]^{c2} [M^0 L^1 T^0]$$

Equating the powers of M, L, and T on both sides, we get

Power of M, c_2= (0)

Power of L, a_2 = (0)

Power of T, b_2 = (-1)

Substituting the values of a_1, b_1 and c_1 in equation (5.6)

$\pi_2 = (V)^0 (D)^{-1}(\rho)^0 k$

$\pi_2 = \frac{k}{D}$

Similarly for the third π-term, we get

$\pi_3 = V^{a3} D^{b3} \rho^{c3} F_D$

$[M^0 L^0 T^0] = [M^0 L^1 T^{-1}]^{a3} . [M^0 L^1 T^0]^{b3} [M^1 L^{-3} T^0]^{c3} [M^1 L^1 T^{-2}]$

Equating the powers of M, L, and T on both sides, we get

Power of M, $c_3 = (-1)$

Power of L, $a_3 = (-2)$

Power of T, $b_3 = (-2)$

Substituting the values of a_1, b_1 and c_1 in equation (5.7)

$\pi_3 = (V)^{-2}(D)^{-2}(\rho)^{-1} F_D$

$\pi_3 = \frac{F_D}{\rho V^2 D^2}$

$\pi_3 = \frac{F_D}{\frac{1}{2}\rho A V^2}$

The dimension form

$\pi_1 = \frac{\mu}{\rho V D} = R_e$

$\pi_2 = \frac{k}{D}$

$$\pi_3 = \frac{F_D}{\frac{1}{2}\rho A V^2}$$

$$\frac{F_D}{\frac{1}{2}\rho A V^2} = C(R_e)^{n_1}\left(\frac{k}{D}\right)^{n_2}$$

The values of constant C as exponents n_1 *and* n_2 are obtained for the Figure (1), (2) and final correlation graph (4) is given below.

5.3 DIMENSIONLESS FORM

(i) Dimensionless terms: $\frac{F_D}{\frac{1}{2}\rho A V^2} = C(Re)^{n_1}\left(\frac{k}{D}\right)^{n_2}$

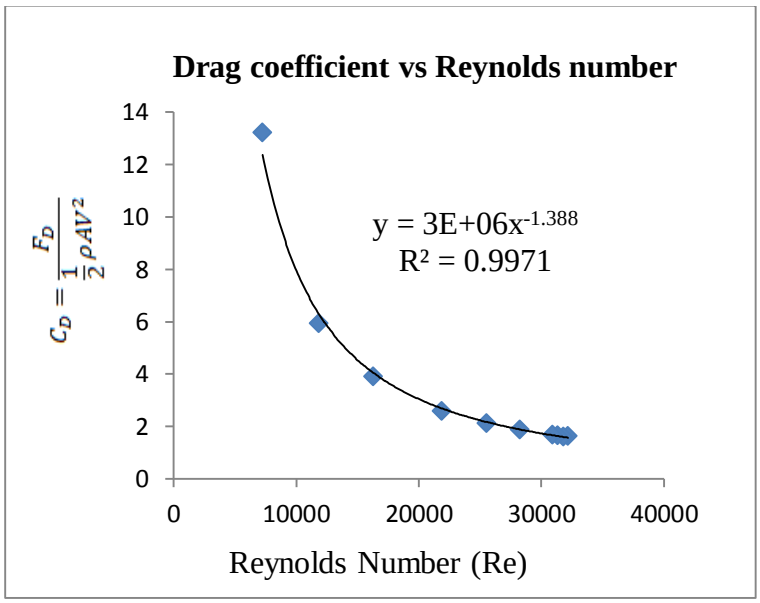

Fig.5.1 The relationship between drag coefficient and Reynolds number.

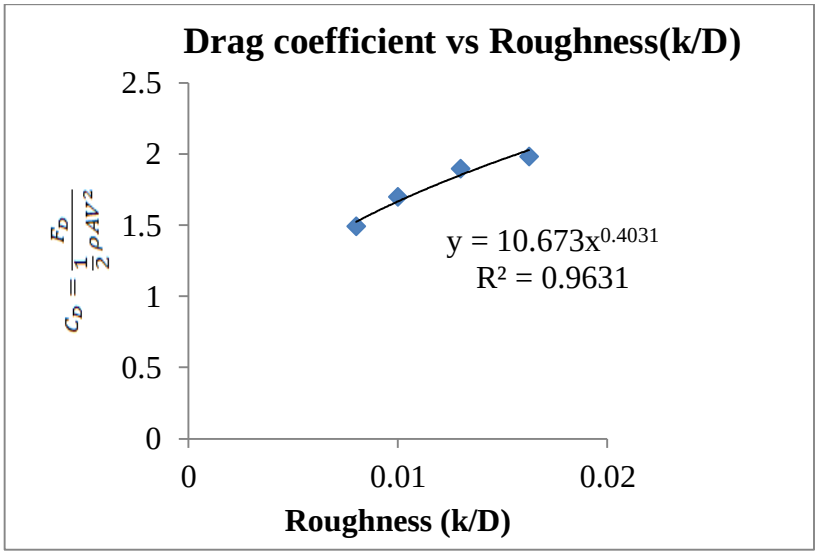

Fig.5.2 Relationship between drag coefficient and Roughness

From the graphical plot in Figure 5.1(i) and Figure 5.2(ii) we get the value of n_1= (-1.388) and n_2= 0.4031. Then found out the value of $x = (R_e)^{n_1}\left(\frac{k}{D}\right)^{n_2}$ and plot the graph between drag force (i.e. effect of Reynolds number and effect of roughness) and x. in Figure 5.3.

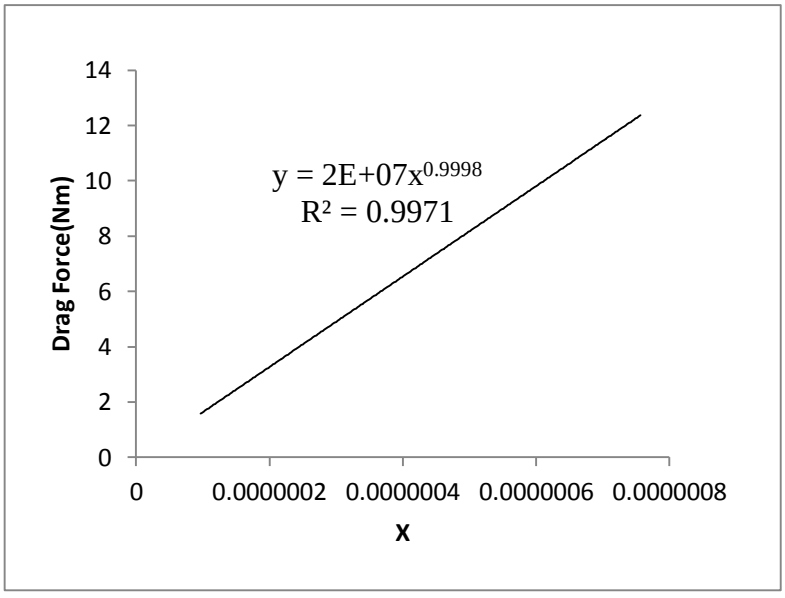

Fig.5.3: The relationship between drag coefficient and effect Reynolds number & effect of roughness.

Table.5.1 Details of correlation constant parameters.

Roughness(k)	Diameter(D)	k/D	
0.000325	0.025	0.0130	
0.000260	0.025	0.0104	
0.000200	0.025	0.0080	
0.000160	0.025	0.0064	
0.000325	0.02	0.0162	
0.000260	0.02	0.0130	1st constant
0.000200	0.02	0.0100	2nd constant
0.000160	0.02	0.0080	3rd constant
0.000325	0.015	0.0216	
0.000260	0.015	0.0173	
0.000200	0.015	0.0133	
0.000160	0.015	0.0106	
0.000325	0.0125	0.0260	
0.000260	0.0125	0.0208	
0.000200	0.0125	0.0160	
0.000160	0.0125	0.0128	

Table.5.2 Details of dimensionless parameters of the experimental runs (Roughness=0.000260m)

Velocity(V)	Diameter(D)	Reynolds number	Drag Force(F_D)	Drag coefficient (C_D)
25.81	0.02	32190.07234	0.608012	1.633587
25.48	0.02	31778.49838	0.588399	1.622105
25.14	0.02	31354.45248	0.583496	1.652391
24.8	0.02	30930.40659	0.580554	1.689448
22.64	0.02	28236.46795	0.539366	1.883373
20.46	0.02	25517.58543	0.500139	2.138382
17.54	0.02	21875.7795	0.446203	2.595845
13.07	0.02	16300.82315	0.372653	3.904441
9.5	0.02	11848.34123	0.299103	5.931699
5.84	0.02	7283.611873	0.252031	13.22616

Table.5.3 Details of dimensionless parameters of constant velocity =20.46m/s & diameter =0.02m

Roughness(k)	k/d	Reynolds number	Drag Force (F_D)	Drag Coefficient (C_D)
0.000325	0.01625	25517.58543	0.243205	1.039841
0.00026	0.013	25517.58543	0.225553	0.964369
0.0002	0.01	25517.58543	0.20594	0.88051
0.00016	0.008	25517.58543	0.196133	0.838581

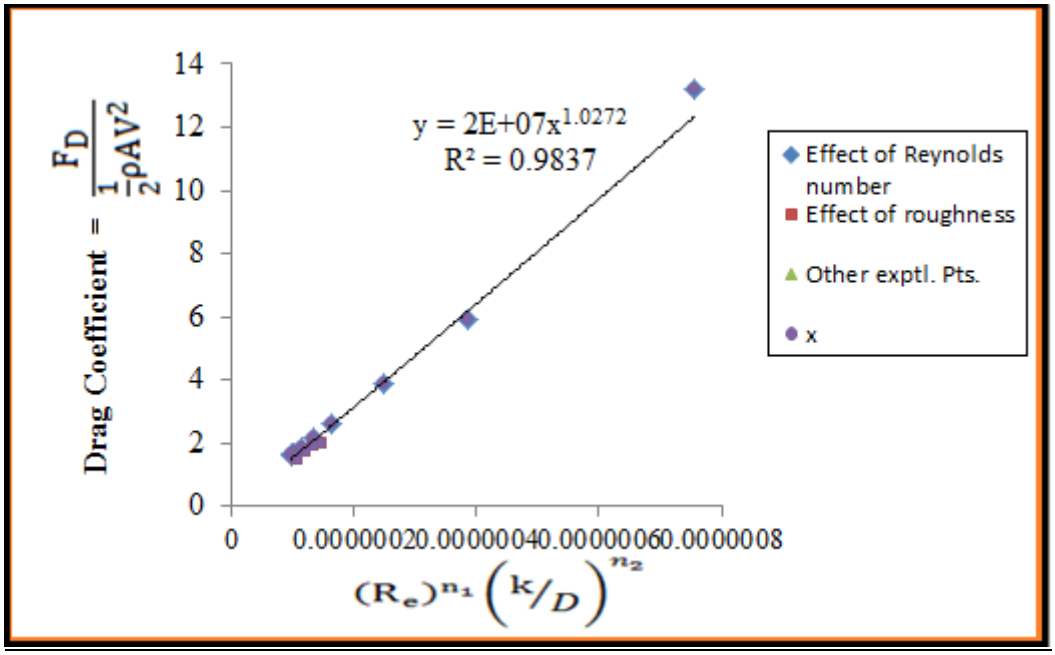

Fig.5.4 the relationship between drag coefficient and effect Reynolds numbers, effect of roughness and other explicit data

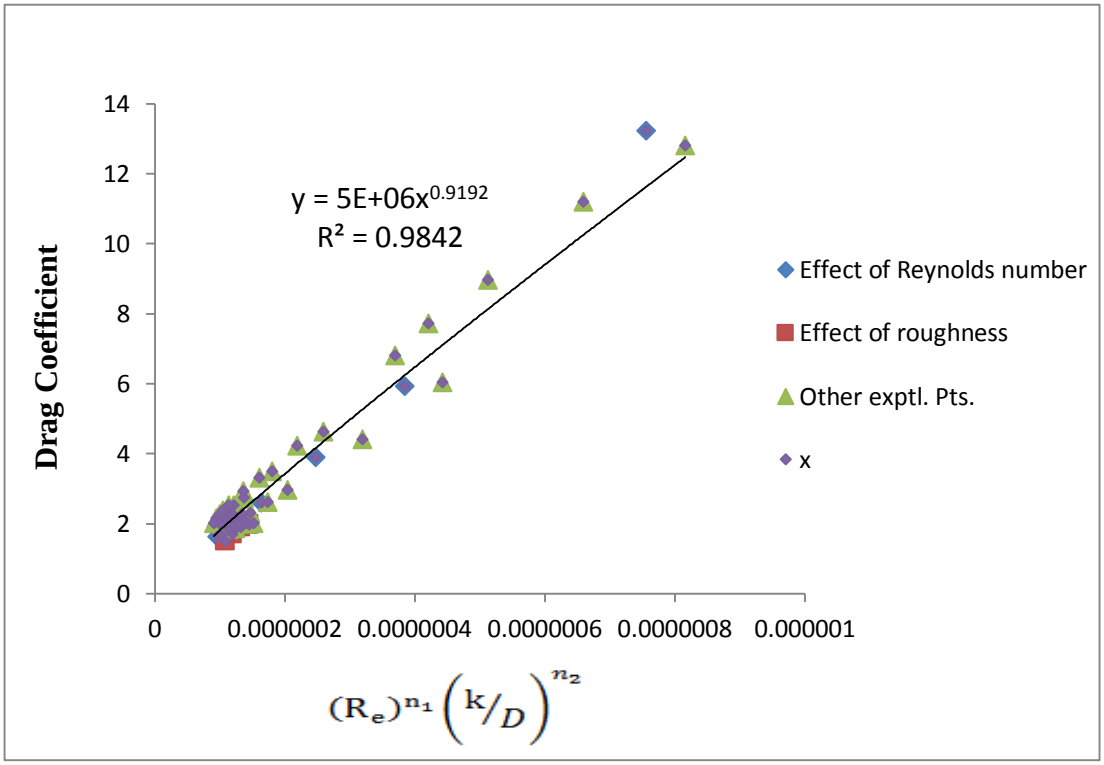

Fig.5.5 Final correlation plot between the drag parameter with system parameter

it is clearly seen that from the graph, it is plotted between the predicted Drag coefficient verses correlation data for rough cylindrical bodies. In this case, it is found that in Figure 5.3 both drag coefficient vs. effect of reynolds number and effect of roughness agrees perfectly and also gives a satisfactory result along appropriately with determination or Regression coefficient is R^2=0.99. Similarly, the comparison occurs in between the drag coefficient vs. effect of reynolds number, effect of roughness and other explicit data has been shown in Figure 5.4 for experimental data and R^2=0.98. Respectively the Regression coefficient R^2 for all these data sets are found to be 0.99 and 0.98 and these all are gives a satisfactory results. Therefore from the above Figure it is clearly shown that the present model gives a better drag coefficient result. In the dimensionless correlation graph mean % error is 4.067.

CHAPTER VI
ESTABLISHMENT OF CORRELATION

6.1 CORRELATION DEVELOPMENT

The Drag coefficient is defined as by a relationship between the drag force F_D and the $\frac{1}{2}\rho AV^2$. Drag coefficient depends on the drag force, free stream velocity and projected area. For this experiment data sets are collected by experimentation. So in the present work for regression analysis, dimensional analysis is used. In this dimensional analysis the variables are used two types, i.e. dependent and independent variables. All the variables are analyzed through the experiments with keeping different diameter, velocity and roughness. Then a model is required for rough cylindrical bodies which should consider the variable geometric such as diameter, velocity and roughness parameters.

6.1.1 Data processing

The experimental data for drag force with varying diameter, roughness size and free stream velocity have been collected. From the literature study, it is seen that the drag coefficient of a rough cylindrical bodies varies surface area, velocity and roughness. They are found to be function of geometric parameters, flow parameters and surface parameters. All are dimensionalised. These data have been processed to predict the output viz. drag force by the following methods: (i) Dimensional analysis.

6.2 DIMENSIONAL ANALYSIS

The following system variables which are likely to impact the output of the system viz. diameter, roughness and velocity have been considered in the development of the correlations:

Dimensional terms: $F_D = C(V^{n_1})(D^{n_2})(k^{n_3})$

Drag force (F_D)

Velocity (V)

Diameter (D)

Roughness (k)

The Geometric parameter is Diameter and Flow parameter is Reynolds no. It is in the following form $F_D = f(V, D, k)$

The variation of drag force has been found out for four cylinders of different diameters and roughness. The variations of drag force in terms of drag force are plotted for different roughness in Figure (6.1). It is seen that, when roughness is increased as drag force increases because drag force is less in smooth and very in rough surface. In Figure (6.2) the variation of drag force are plotted for different velocity. When velocity increases, drag force will increase. In Figure (6.3) the variation of drag force are plotted for different diameter. It seen that the drag force is increases with increases in diameter, because the surface area is increases.

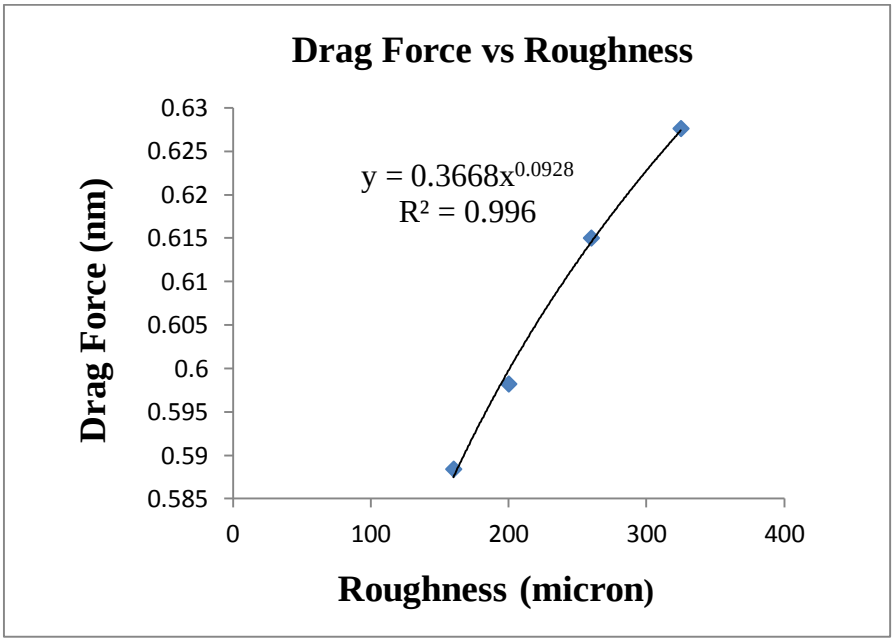

Fig.6.1 The relationship between drag force and roughness

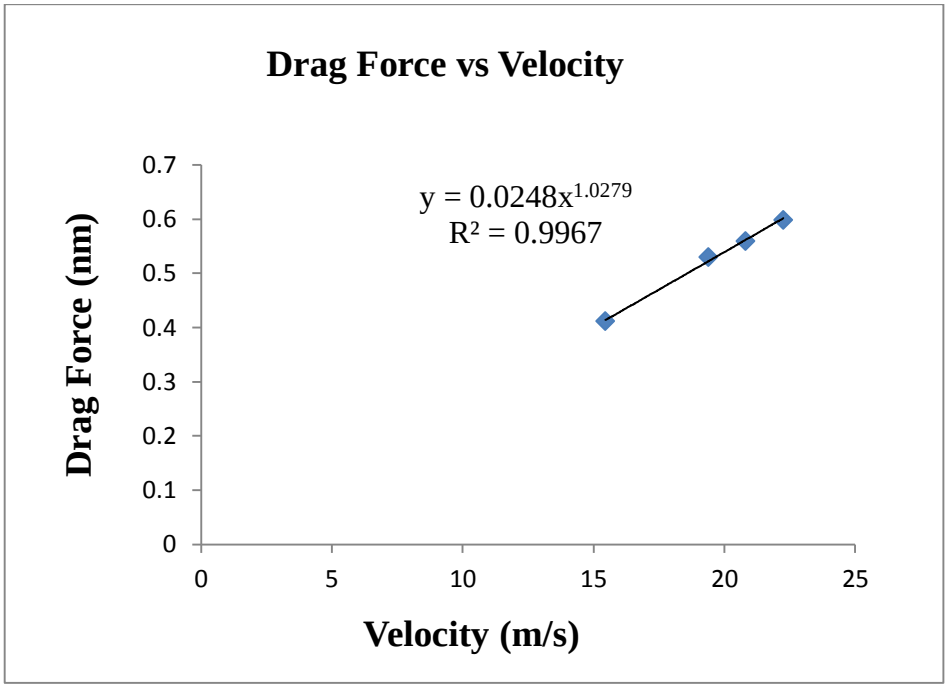

Fig. 6.2 The relationship between Drag force and Velocity

.

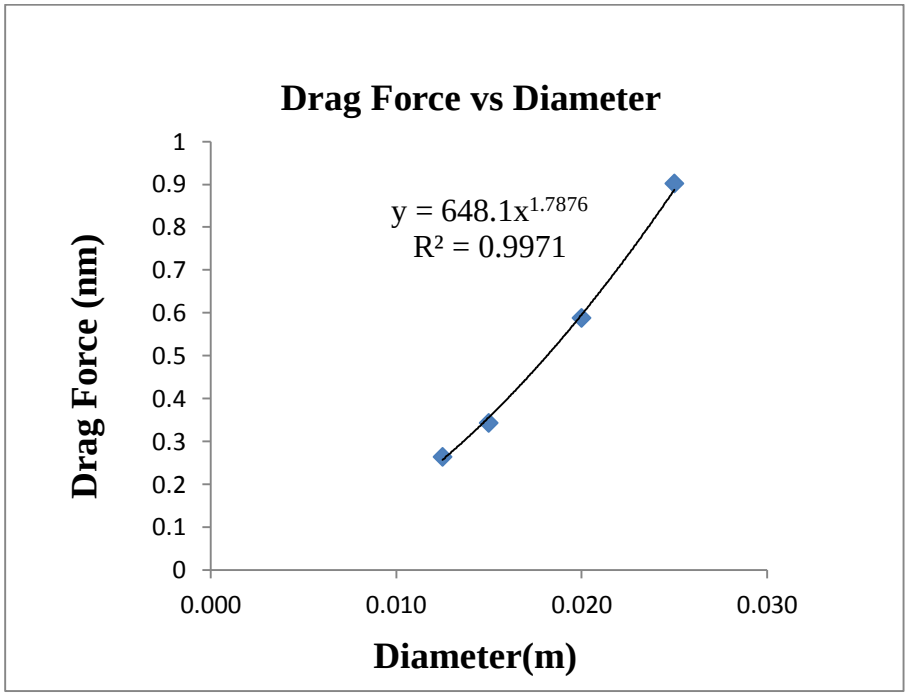

Fig. 6.3 The relationship between Drag force and Diameter

Table.6.1 Details of dimensional parameters of the experimental runs.

Roughness	Velocity	Diameter	X	F_D	F_D	F_D	Drag force (F_D)	exponent	predicted F_D	% error
325	22.26	0.02	0.038	0.62			0.6272	0.0931	0.61198	2.4
260	22.26	0.02	0.037	0.61			0.6150		0.59941	2.5
200	22.26	0.02	0.036	0.59			0.5982		0.58496	2.2
160	22.26	0.02	0.035	0.58			0.5883		0.57295	2.6
260	22.26	0.02	0.037		0.59		0.5983	1.0413	0.59941	0.1
260	20.80	0.02	0.034		0.55		0.5593		0.55850	0.1
260	19.39	0.02	0.032		0.52		0.5295		0.51911	1.9
260	15.46	0.02	0.025		0.41		0.4118		0.40998	0.4
260	22.26	0.0125	0.016			0.26	0.2647	1.8112	0.25565	3.4
260	22.26	0.015	0.022			0.34	0.3432		0.35580	3.6
260	22.26	0.02	0.037			0.58	0.5883		0.59941	1.8
260	22.26	0.025	0.055			0.90	0.9022		0.89830	0.4

For the above three graphs, we get

$n_1 = 0.0928,$

$n_2 = 1.0279,$

$n_3 = 1.7876$

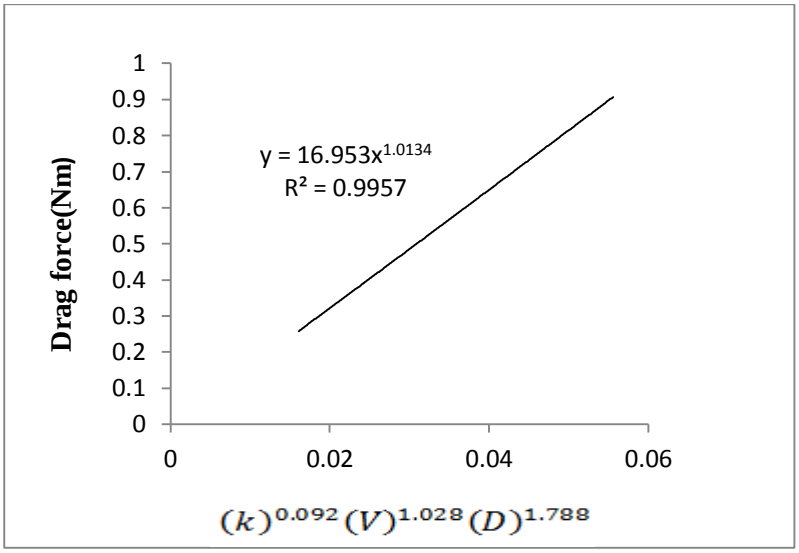

Fig.6.4 The relationship between Drag force and x.

Then found out the value of $x = (V)^{n_1}(D)^{n_2}(k)^{n_3}$ and plot the graph between drag force and x (i.e. effect of velocity, effect diameter and effect of roughness). In Figure 6.4 and put the three values is given i.e. 0.0928, 1.028 and 1.788.

$y = 16.953x^{1.0134}$

$R^2 = 0.99$

In Figure 6.5, the graph between drag forces and $x = (V)^{n_1}(D)^{n_2}(k)^{n_3}$, other correlation data are plotted. The values of exponent are 0.093, 1.042 and 1.813.

$y = 13.582x^{1.0367}$

$R^2 = 0.98$

In Figure 6.6, the graph between drag force and effect of roughness, effect of velocity, effect of diameter and other explicit points.

$y = 10.508x^{0.9463}$

$R^2 = 0.97$

Table.6.2 Details of dimensional parameters of the experimental runs with other explicit points and correlation data

Roughness	Velocity	Diameter	x	Effect of roughness	Effect of velocity	Effect of diameter	Other explicit points	correlation
325	22.26	0.02	0.050927	0.62762				0.62762
260	22.26	0.02	0.049326	0.61501				0.615012
200	22.26	0.02	0.047509	0.5982				0.5982
160	22.26	0.02	0.046016	0.5884				0.588399
260	22.26	0.02	0.049326		0.5984			0.598399
260	20.8	0.02	0.046004		0.5594			0.559365
260	19.39	0.02	0.042801		0.5296			0.529559
260	15.46	0.02	0.03391		0.4119			0.411879
260	22.26	0.0125	0.021287			0.26477		0.26477
260	22.26	0.015	0.029491			0.34323		0.343232
260	22.26	0.02	0.049326			0.5884		0.588399
260	22.26	0.025	0.073512			0.90221		0.902211
325	21.87	0.025	0.07453				0.8924	0.8924
260	21.87	0.025	0.072188				0.88079	0.88079
200	21.87	0.025	0.069528				0.86298	0.86298
160	21.87	0.025	0.067343				0.85317	0.85317
325	21.87	0.025	0.07453				0.87279	0.87279
325	19.39	0.025	0.065856				0.81395	0.81395
325	15.46	0.025	0.052176				0.72647	0.726465
325	21.87	0.0125	0.021582				0.2432	0.2432
325	21.87	0.015	0.0299				0.32362	0.323619
325	21.87	0.02	0.05001				0.57859	0.578592
325	21.87	0.025	0.07453				0.87279	0.87279

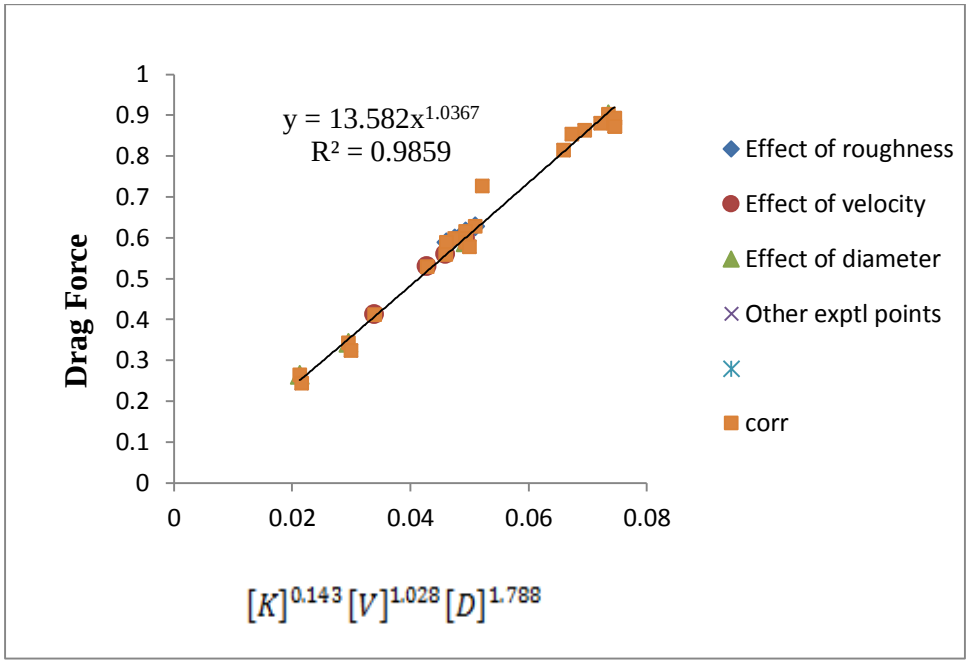

Fig.6.5 relationship between Drag force and effect of k, V, D and other correlation data

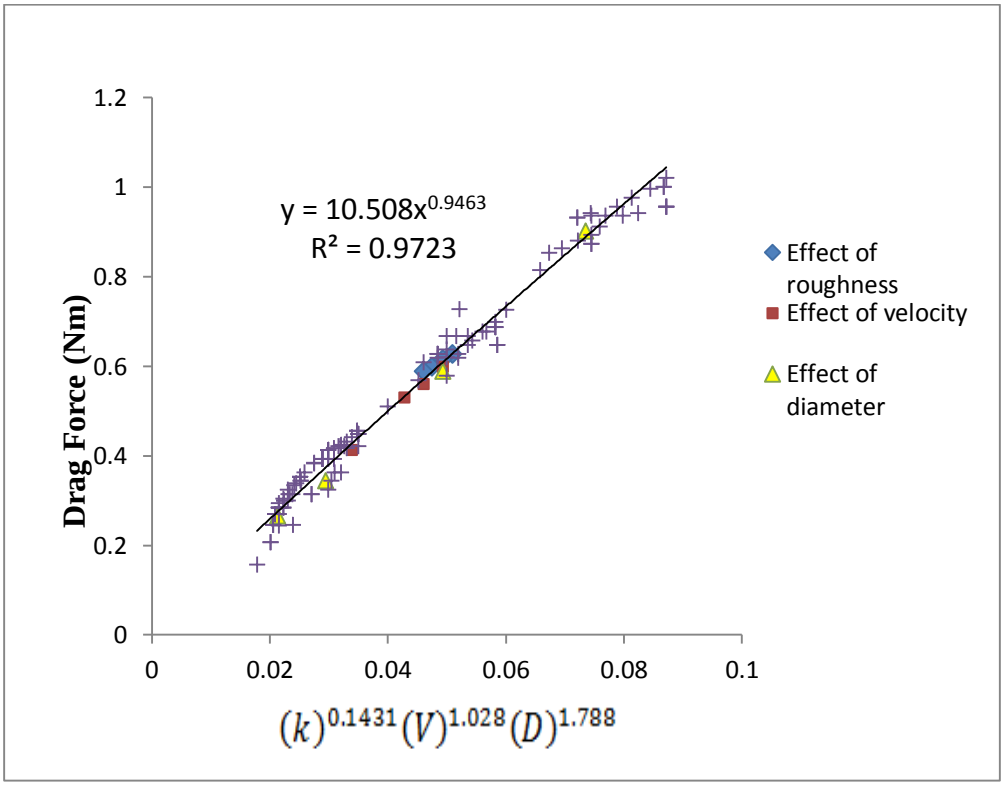

Fig.6.6 relationship between Drag force and effect of k, V, D and other explicit points

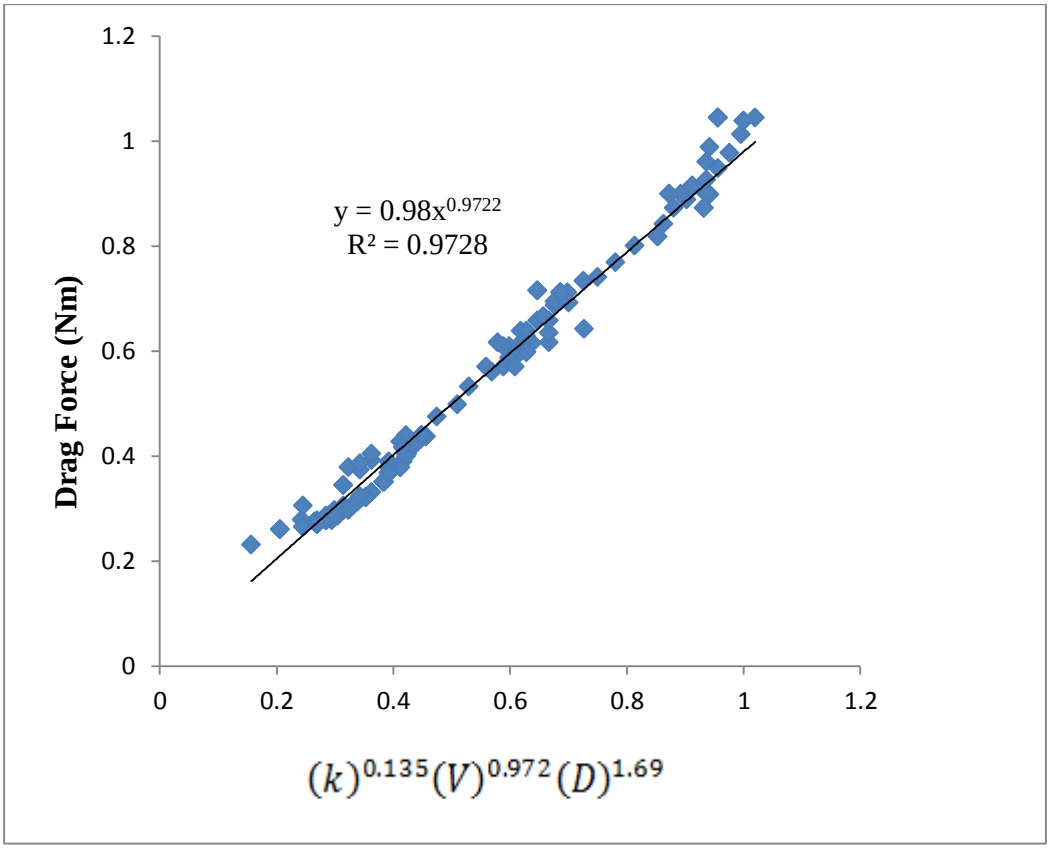

Fig 6.7 Final correlation plots between the drag parameter with system parameters in dimensional data

Then found out the value of $x = (V)^{n_1}(D)^{n_2}(k)^{n_3}$ and plot the graph between drag force and x (i.e. effect of velocity, effect diameter and effect of roughness).

$y = 0.98x^{0.9722}$

$R^2 = 0.972$

it is clearly seen that from the above graph, it is plotted between the predicted Drag force verses correlation data for rough cylindrical bodies. In this case, it is found that in Figure 6.1 both drag force vs. roughness agrees perfectly and also gives a satisfactory result along appropriately with determination or Regression coefficient is R^2=0.996. Similarly, the comparison occurs in between the drag force vs. velocity has been shown in Figure 6.2 for experimental data and R^2=0.9967. Similarly, the comparison occurs in between the drag force vs. diameter has been shown in Figure 6.3 for experimental data and R^2=0.997.

Respectively the Regression coefficient R^2 for all these data sets are found to be 0.99, 0.99, 0.99, 0.99, 0.98, 0.97 and 0.97 and these all are gives a satisfactory results. Therefore from the above Figure it is clearly shown that the dimensional correlation graph gives a better drag force result. In the dimensionlnal correlation graph mean % error is 3.067.

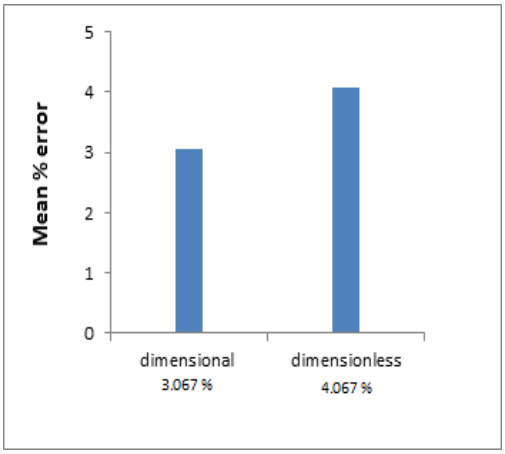

Fig. 6.8 mean percentage error

CHAPTER VII
CONCLUSION

7.1 OVERVIEW

Extensive literature survey has been carried out to study the drag force and pressure distribution of a rough cylindrical bodies. From the literature, it is found that Reynolds number depends upon velocity, diameter or radius and kinematic viscosity. As compare to both methods of drag force, the direct measurement method gives more reliable than the pressure distribution method. From the experimental findings and different plots shown above, the following conclusions can be derived:

- The drag force increases with increase in diameter of the cylinder, because drag force is directly proportional to area of cylinder.
- When flow velocity is increase the drag force increases. But drag coefficient decreases with increase in drag force. Drag coefficient is inversely proportional ti drag force. When diameter, velocity and roughness of the cylinder increases the drag coefficient decreases.
- The drag force increases with increase in roughness and drag coefficient is decreases. In this case, drag force increases with the smooth surface and decreases in rough surface in compare smooth surface and rough surface.
- For a cylinder of particular diameter and roughness, drag force has been found to increase with increase in air velocity.
- Drag coefficient decreases with an increase in Reynolds number for all k/D ratios for a cylinder. But drag force increases with increases in Reynolds number for all k/D ratios for a cylinder. Because Reynolds number depends upon velocity and diameter.

- In pressure distribution method, the diameter increases with their pressure coefficient is very high. In both methods we found drag coefficient in different ways. In direct weighing method we found drag coefficient by the formula but in pressure distribution method we found the drag coefficient by area under the curve.
- The present study under taken can be further extended to study the effect of surface roughness on flow parameters for different shape and configuration of objects.
- The results of pressure distribution profiles clearly show that the flow separates at around 80^0-90^0 on either side of the cylinder from the upstream stagnation point.
- As compare to both methods of drag force, the direct measurement method gives more reliable than the pressure distribution method.
- For a constant Reynolds number, the value of drag coefficient decreases with an increase in k/D ratio of the cylinder.
- In dimensional correlation result is very sensitive, accurate and deterministic. The mean % error of dimensional error is 3.047 %. In dimensionless correlation result is linear with their parameters. The mean % error of dimensionless is 4.047 %.

7.2 SCOPE FOR FUTURE WORK

The present work leaves a wide scope for future investigators to explore many other aspects of an aerodynamic analysis.

- The setup of airflow bench, we investigated the another attachment of wake traverse.
- In this setup we used different diameters of cylinder, in futher studied we used different length, different shapes of models such as sphere, airfoil, rectangular, flat plate etc.

- Another tested of this project is we compare the big setup of wind tunnel and airflow bench.
- The correlation developed may be improved by incorporating more data from cylinder of different geometries.
- The relationship is establised between the drag force and roughness, here the roughness is made dimensionaless by dividing the diameter of the cylinder. The further work can be done by making it by non-dimensional through any one dimensional parameter.

REFFERENCES

1. Roshko, Anatol. "Experiments on the flow past a circular cylinder at very high Reynolds number." Journal of Fluid Mechanics 10.03 (1961): 345-356.
2. Alridge, T. R., B. S. Piper, and J. C. R. Hunt. "The drag coefficient of finite-aspect-ratio perforated circular cylinders." Journal of Wind Engineering and Industrial Aerodynamics 3.4 (1978): 251-257.
3. Achenbach, E., and E. Heinecke. "On vortex shedding from smooth and rough cylinders in the range of Reynolds numbers 6×10^3 to 5×10^6." Journal of fluid mechanics 109 (1981): 239-251.
4. Merrick, Ryan, and Girma Bitsuamlak. "Control of flow around a circular cylinder by the use of surface roughness: A computational and experimental approach." Journal of Fluid Mechanics (1982) 123, 363-378.
5. Bearman, P. W., and J. K. Harvey. "Control of circular cylinder flow by the use of dimples." AIAA journal 31.10 (1993): 1753-1756.
6. Shih, W. C. L., et al. "Experiments on flow past rough circular cylinders at large Reynolds numbers." Journal of Wind Engineering and Industrial Aerodynamics 49.1 (1993): 351-368.
7. Mittal, R., and S. Balachandar. "Effect of three-dimensionality on the lift and drag of nominally two dimensional cylinders." Physics of Fluids (1994-present) 7.8 (1995): 1841-1865.
8. Williamson, Charles HK. "Vortex dynamics in the cylinder wake." Annual review of fluid mechanics 28.1 (1996): 477-539.

9. Bouak, F., and J. Lemay. "Use of the wake of a small cylinder to control unsteady loads on a circular cylinder." Journal of Visualization 4.1 (2001): 61-72.
10. Grosche, F-R., and G. E. A. Meier. "Research at DLR Göttingen on bluff body aerodynamics, drag reduction by wake ventilation and active flow control."Journal of Wind Engineering and Industrial Aerodynamics 89.14 (2001): 1201-1218.
11. Protas, B., and J. E. Wesfreid. "Drag force in the open-loop control of the cylinder wake in the laminar regime." Physics of Fluids (1994-present) 14.2 (2002): 810-826.
12. Tsutsui, T., and T. Igarashi. "Drag reduction of a circular cylinder in an air-stream." Journal of Wind Engineering and Industrial Aerodynamics 90.4 (2002): 527-541.
13. Mahbub Alam, Md, M. Moriya, and H. Sakamoto. "Aerodynamic characteristics of two side-by-side circular cylinders and application of wavelet analysis on the switching phenomenon." Journal of Fluids and Structures 18.3 (2003): 325-346.
14. Lee, Sang-Joon, Sang-Ik Lee, and Cheol-Woo Park. "Reducing the drag on a circular cylinder by upstream installation of a small control rod." Fluid dynamics research 34.4 (2004): 233-250.
15. Mittal, Sanjay, and Saurav Singh. "Vortex-induced vibrations at subcritical Re. "Journal of Fluid Mechanics 534 (2005): 185-194.
16. Bergmann, Michel, Laurent Cordier, and Jean-Pierre Brancher. "Drag minimization of the cylinder wake by trust-region proper orthogonal decomposition." Active Flow Control. Springer Berlin Heidelberg, (2007): 309-324.
17. Lyotard, Nicolas, et al. "Polymer and surface roughness effects on the drag crisis for falling spheres." The European Physical Journal B 60.4 (2007): 469-476.

18. Pasto, S. "Vortex-induced vibrations of a circular cylinder in laminar and turbulent flows." Journal of Fluids and Structures 24.7 (2008): 977-993.
19. Zheng, Z. C., and N. Zhang. "Frequency effects on lift and drag for flow past an oscillating cylinder." Journal of Fluids and Structures 24.3 (2008): 382-399
20. Triyogi, Y., D. Suprayogi, and E. Spirda. "Reducing the drag on a circular cylinder by upstream installation of an I-type bluff body as passive control. "Proceedings of the Institution of Mechanical Engineers, Part C: Journal of Mechanical Engineering Science 223.10 (2009): 2291-2296.
21. Libii, Josué Njock. "Using wind tunnel tests to study pressure distributions around a bluff body: the case of a circular cylinder." World Transactions on Engineering and Technology Education 8.3(2010)
22. Mohammad and Islam et al. "Reduction of Drag Force of a Cylinder by Attaching Cylindrical Rings", Proceedings of the 13th Asian Congress of Fluid Mechanics, (2010), Dhaka, Banglades.
23. Hodžić, Nedim, and Rasim Begagić. "Experimental investigation of boundary layer separation influence of pressure distribution on cylinder surface in wind tunnel armfield C15-10." (2011)
24. D'auteuil, Annick, Guy L. Larose, and Steve J. Zan. "Wind turbulence in speed skating: measurement, simulation and its effect on aerodynamic drag." Journal of Wind Engineering and Industrial Aerodynamics 104 (2012): 585-593.
25. M.Vignesh Kumar, Pillai et.al. "Drag characteristics of circular cylinder with various roughness for higher Reynolds number." VI National Conference on Wind Engineering, (2012), 14-15

26. Richter, Andreas, and Petr A. Nikrityuk. "Drag forces and heat transfer coefficients for spherical, cuboidal and ellipsoidal particles in cross flow at sub-critical Reynolds numbers." International Journal of Heat and Mass Transfer 55.4 (2012): 1343-1354.
27. Butt, U., and C. Egbers. "Aerodynamic Characteristics of Flow over Circular Cylinders with Patterned Surface." J. Materials, Mechanics, Manufacturing 1.2 (2013).
28. Toukir Islam and S.M. Rakibul Hassan, "Experimental and Numerical Investigation of Flow over a Cylinder at Reynolds Number 10^5", Journal of Modern Science and Technology, (2013) 1. 1 .52-60.
29. . Tamayol, A., et al. "Low Reynolds number flows across ordered arrays of micro-cylinders embedded in a rectangular micro/minichannel." International Journal of Heat and Mass Transfer 58.1 (2013): 420-426.

PUBLICATIONS FROM THE WORK

A: Published

1. Monalisa Mallick, A. Kumar (2014) "Study on Drag Coefficient for the Flow Past a Cylinder," International Journal of Civil Engineering Research, vol.5, pp. 301-306
2. Monalisa Mallick, A. Kumar (2014) "Experimental Investigation of Flow Past A Rough Surfaced Cylinder," International Journal of Engineering Research and Applications (IJERA).